

**Fig. 1.** *JAK2*<sup>V617F</sup>-positive ET patients exhibit distinct bone marrow morphological changes. **A:** A representative of ET *JAK2*<sup>V617F</sup>-positive cases showing hyperplasia of megakaryocytes (H&E stain  $\times 200$ ). **B,C:** Dysplastic changes of megakaryocytes (multinucleated and binucleated cells). **D:** Small sized megakaryocytes (H&E stain  $\times 1,000$ ).

7 to 15 years (median 14 Years). The median hemoglobin levels, white blood cell counts, and platelet counts were 19 g/dl (range 15.8–21.8 g/dl),  $15.6 \times 10^9/L$  (range  $6.7\text{--}19.2 \times 10^9/L$ ), and  $229 \times 10^9/L$  (range  $114\text{--}529 \times 10^9/L$ ), respectively. Cytogenetic analysis of bone marrow revealed normal karyotype in all ET and PV patients.

#### Mutations of Candidate Genes in Pediatric ET and PV Patients

We analyzed the sequences of several candidate genes in ET and PV patients. Through *allele specific* PCR combined with sequence analysis, a G  $\rightarrow$  T alteration was detected at codon 617 in exon 14 of *JAK2* (which results in a substitution of valine for phenylalanine) in two out of nine (22%) ET patients and one out of four (25%) PV patients (Fig. 2; Table I). We also found a point mutation (C to T) at codon 1230 in exon 12 of *ASXL1* in one (11%) out of nine ET patients and in one (25%) out of four PV patients, which results in amino acid conversion from serine to phenylalanine. This mutation was not included in the public database (Fig. 3) (Table I), but 3 out of 30 healthy Japanese control were found to harbor this mutation, indicating that *ASXL1* (p.S1230F) mutation could be encountered as SNP. The occurrence of *TET2* alterations was also investigated, synonymous point mutations c.3117G>A (S1039S) and c.4140T>C (H1380H) were detected in ET patients and confirmed in healthy controls. After exclusion of common SNPs present in public databases and/or detected in 30 healthy controls survey, no other *TET2*

mutations could be found in ET and PV patients. None of the ET and PV patients showed genetic alterations in *JAK2* exon 12, *CBL*, *IDH1*, and *IDH2* genes. No *MPL* mutations were detected among ET pediatric patients included in this cohort (Table I).

#### DISCUSSION

An increasing interest in *BCR-ABL1*-negative MPN in childhood has emerged recently, with a particular emphasis on ET and PV. Considering the low incidence of ET and PV among children compared to the adult patients, we believe that the new biological insights will help us to validate new diagnostic and therapeutic guidelines for childhood MPN. We reported nine cases of ET with median age 11.5 years (range 1.5–15 years) and high platelet counts (median:  $1.827 \times 10^9/L$ ; range:  $923\text{--}2.900 \times 10^9/L$ ). *JAK2*<sup>V617F</sup>-positive ET patients had a predominant increase in the leucocytic counts. Six out of nine ET patients received anti-platelet drug (Aspirin) (Table I). Four patients with PV were also included in this study; the age at diagnosis for those patients ranged from 7 to 15 years (median 14 years) presented with high hematocrit values (range 46.2–71.5%). The PV patient who had a *JAK2*<sup>V617F</sup> mutation, showed a significant increase in hemoglobin, hematocrit level, and WBCs counts compared to *JAK2*<sup>V617F</sup>-negative PV patients. Phlebotomy was performed for this patient in order to remove the excess cellular elements and to decrease the hematocrit value, while the other three patients with PV were not given any therapy (Table I). These data are consistent with previous reports mentioned that most children with ET

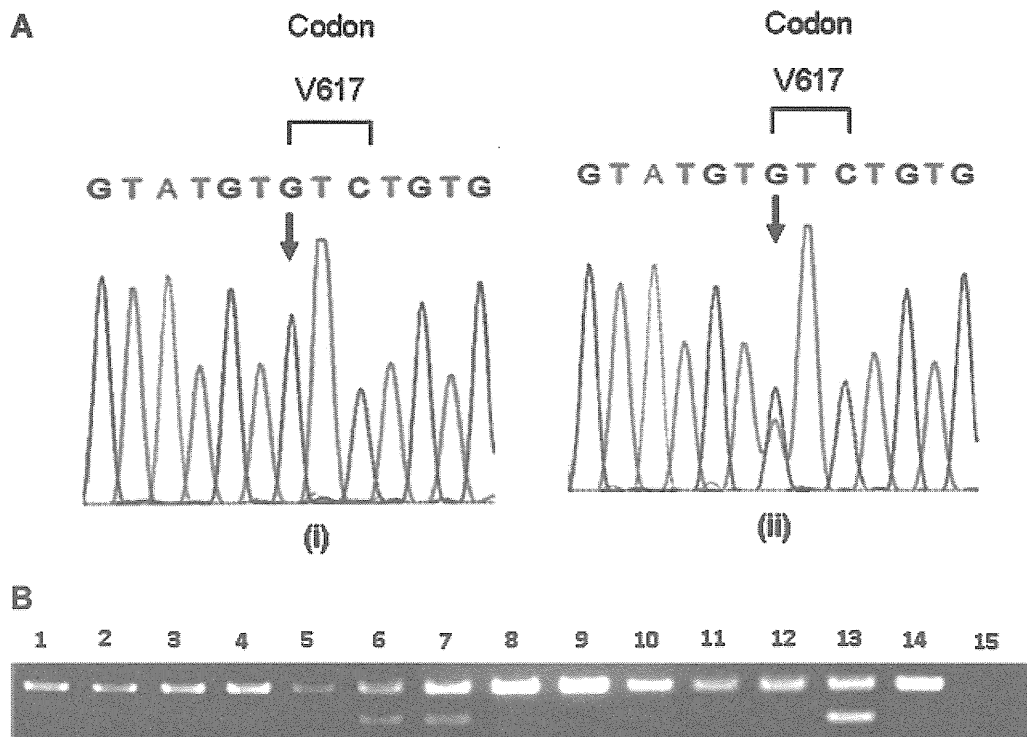


**Fig. 2.**  $JAK2^{V617F}$  mutation among PV and ET pediatric patients. **A:** Sequence traces. Showing mutation analysis of  $JAK2$  gene (i) Nucleotide sequences and corresponding amino acid sequences of  $JAK2$  wild-type (ii) G to T  $JAK2$  mutation in two ET patients and one PV patient. Arrows directed to the relevant base. **B:** Allele-specific PCR displayed results of ET and PV cases. A 203-bp (lower band) indicates mutant DNA with  $JAK2^{V617F}$  mutation while a 364-bp (upper band) indicates wild-type and used as internal control. Lanes 1–9: ET cases; lanes 10–13: PV cases; lane 14: healthy volunteer (negative control); lane 15: no template; lanes 6, 7, and 13: V617F-positive patients.

are characterized by young age and high platelet counts, nevertheless, almost all PV pediatric patients presenting with high hematocrit levels [21,22].

Identification of  $JAK2^{V617F}$  as a biological marker for PV and ET has improved our understanding of the molecular pathogenesis in these disorders. Previous studies of  $JAK2^{V617F}$  have indicated that its prevalence within childhood ET is variable [16,21,23]. In agreement with Randi's report [23] we showed that 22% of pediatric patients with ET carried  $JAK2^{V617F}$  mutation. On the other hand, we found that 25% of PV patients had  $JAK2^{V617F}$ , consistently with that reported by Teofili et al. [16]. In addition to the sequencing method used in this study, we confirmed  $JAK2^{V617F}$  mutation by allele-specific PCR, which is considered a highly sensitive technique to detect this mutational type [24]. In a previous study employing the same technique [16], a higher frequency of  $JAK2^{V617F}$  mutation was detected in 7 cases (39%) of 18 sporadic pediatric ET patients. In line with other observations [21,23], our results showed that childhood incidence of  $JAK2^{V617F}$  mutation in ET and PV is lower than adulthood forms. Interestingly,  $JAK2^{V617F}$ -positive ET patients exhibit distinct histopathological changes of their bone marrow compared to  $JAK2^{V617F}$ -negative patients (who showed only an elevated number of megakaryocytes) including the presence of megakaryocytes with small size and dysplastic features (multinucleated and binucleated form), implying that it might possible to improve the diagnostic ability by integrated classification scheme including the molecular and bone marrow histopathologic findings.

*Pediatr Blood Cancer* DOI 10.1002/pbc

However, these provisional speculations should be confirmed in the subsequent cohorts.

Differently from adult patients, we could not find any alteration in exon 12 of  $JAK2$  among V617F-negative MPN pediatric population, while another report showed that two patients had  $JAK2$  exon 12 out of eight pediatric PV cases [25].

Previous data suggested that  $TET2$  mutation could be acquired before  $JAK2^{V617F}$  in adult MPN [11]. Tefferi [26] reported that  $CBL$  mutation might occur in post-ET/PV fibrotic phase, while  $IDH$  mutations are relatively frequent in blast- but not in chronic-phase of MPN. Our cohort shows that no patient (ET or PV) harbors,  $CBL$ ,  $IDH1$ ,  $IDH2$ , and  $MPL$  mutations, suggesting these genetic alterations are relatively rare to occur in childhood MPN. In our study, none of the patients had a positive family history for ET or PV. However, it has been recently demonstrated that patients diagnosed as familial MPN with thrombocytosis might harbor  $JAK2$  or  $MPL$  mutations which are not considered as the primary pathogenetic lesions. By contrast, alterations of  $MPL$  or thrombopoietin ( $THPO$ ) genes are diseases causing defects in hereditary thrombocytosis [27]. The molecular delineation of PV revealed that  $JAK2^{V617F}$  mutation has a pathogenetic role in this disorder. Nevertheless, primary familial congenital polycythemia is caused by mutations in the Epo receptor ( $EPOR$ ) gene [28]. Moreover, alteration of oxygen-sensing pathway has been shown to be involved in the pathogenesis of the congenital forms of erythrocytosis [29]. Specifically, mutations in the genes encoding VHL, PHD2, and

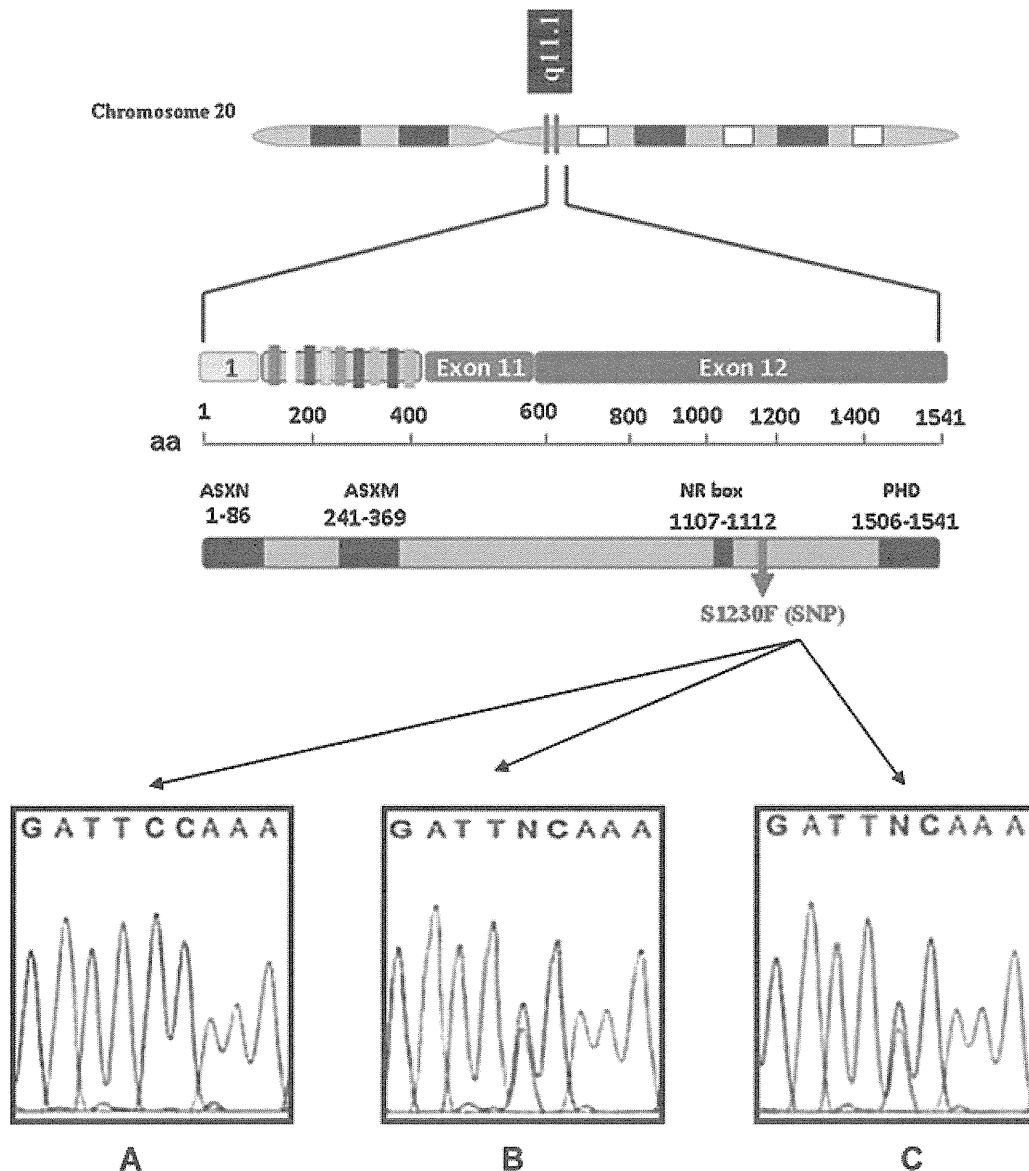


**Fig. 3.** Schematic representation of *ASXL1* showing its chromosomal location, principle functional, and conserved domains. A missense p.S1230F mutation is indicated by red vertical arrows. Nucleotide sequence showing wild-type (A) and mutant *ASXL1* in ET (B) and PV (C) patients.

HIF-2 $\alpha$  have been detected in patients with familial erythrocytosis [30–32].

Here, we have described a missense mutation at codon 1230 in exon 12 of *ASXL1* gene in ET and PV patients that has not been reported before (Fig. 3). We have identified this mutation in healthy Japanese volunteers. Therefore, we conclude that this variation represents a SNP. Previous studies on adulthood MPN showed that *ASXL1* mutation was found in association with *JAK2*<sup>V617F</sup> mutation in PV [33] and was identified as a sole lesion in ET [13]. Large cohort is highly required to better define the occurrence of other genetic alterations that might contribute to the pathophysiology of childhood MPN. In conclusion, our findings provide further evidence that *JAK2* mutations in childhood ET and PV are not as frequent as reported in adulthood ET and PV. Given

*Pediatr Blood Cancer* DOI 10.1002/pbc

the presence of MPN without *JAK2/MPL/ASXL1/TET2/IDH1/IDH2* mutations, it indicates the existence of other alternative unidentified mutations which may contribute to the pathogenesis of childhood MPN.

**REFERENCES**

1. Dameshek W. Some speculations on the myeloproliferative syndromes. *Blood* 1951;6:372–375.
2. Patnaik MM, Tefferi A. The complete evaluation of erythrocytosis: Congenital and acquired. *Leukemia* 2009;23:834–844.
3. Baxter EJ, Scott LM, Campbell PJ, et al. Acquired mutation of the tyrosine kinase *JAK2* in human myeloproliferative disorders. *Lancet* 2005;365:1054–1061.
4. James C, Ugo V, Le Couedic JP, et al. A unique clonal *JAK2* mutation leading to constitutive signalling causes polycythaemia vera. *Nature* 2005;434:1144–1148.
5. Kralovics R, Passamonti F, Buser AS, et al. A gain-of-function mutation of *JAK2* in myeloproliferative disorders. *N Engl J Med* 2005;352:1779–1790.

6. Levine RL, Wadleigh M, Cools J, et al. Activating mutation in the tyrosine kinase JAK2 in polycythemia vera, essential thrombocythemia, and myeloid metaplasia with myelofibrosis. *Cancer Cell* 2005;7:387–397.
7. Scott LM, Tong W, Levine RL, et al. JAK2 exon 12 mutations in polycythemia vera and idiopathic erythrocytosis. *N Engl J Med* 2007;356:459–468.
8. Pietra D, Li S, Brisci A, et al. Somatic mutations of JAK2 exon 12 in patients with JAK2 (V617F)-negative myeloproliferative disorders. *Blood* 2008;111:1686–1689.
9. Tefferi A, Vainchenker W. Myeloproliferative neoplasms: Molecular pathophysiology, essential clinical understanding, and treatment strategies. *J Clin Oncol* 2011;29:573–582.
10. Levine RL, Pardanani A, Tefferi A, et al. Role of JAK2 in the pathogenesis and therapy of myeloproliferative disorders. *Nat Rev Cancer* 2007;7:673–683.
11. Tefferi A, Lim KH, Levine R. Mutation in TET2 in myeloid cancers. *N Engl J Med* 2009;361:1117; author reply 1117–1118.
12. Schaub FX, Looser R, Li S, et al. Clonal analysis of TET2 and JAK2 mutations suggests that TET2 can be a late event in the progression of myeloproliferative neoplasms. *Blood* 2010;115:2003–2007.
13. Carubbia N, Murati A, Trouplin V, et al. Mutations of ASXL1 gene in myeloproliferative neoplasms. *Leukemia* 2009;23:2183–2186.
14. Grand FH, Hidalgo-Curtis CE, Ernst T, et al. Frequent CBL mutations associated with 11q acquired uniparental disomy in myeloproliferative neoplasms. *Blood* 2009;113:6182–6192.
15. Tefferi A, Lasho TL, Abdel-Wahab O, et al. IDH1 and IDH2 mutation studies in 1473 patients with chronic-, fibrotic- or blast-phase essential thrombocythemia, polycythemia vera or myelofibrosis. *Leukemia* 2010;24:1302–1309.
16. Teofili L, Giona F, Martini M, et al. Markers of myeloproliferative diseases in childhood polycythemia vera and essential thrombocythemia. *J Clin Oncol* 2007;25:1048–1053.
17. Teofili L, Foa R, Giona F, et al. Childhood polycythemia vera and essential thrombocythemia: Does their pathogenesis overlap with that of adult patients? *Haematologica* 2008;93:169–172.
18. Tefferi A, Thiele J, Vardiman JW. The 2008 World Health Organization classification system for myeloproliferative neoplasms: Order out of chaos. *Cancer* 2009;115:3842–3847.
19. Kim HJ, Jang JH, Yoo EH, et al. JAK2 V617F and MPL W515L/K mutations in Korean patients with essential thrombocythemia. *Korean J Lab Med* 2010;30:474–476.
20. Gelsi-Boyer V, Trouplin V, Adelaide J, et al. Mutations of polycomb-associated gene ASXL1 in myelodysplastic syndromes and chronic myelomonocytic leukaemia. *Br J Haematol* 2009;145:788–800.
21. El-Moneim AA, Kratz CP, Boll S, et al. Essential versus reactive thrombocythemia in children: Retrospective analyses of 12 cases. *Pediatr Blood Cancer* 2007;49:52–55.
22. Thiele J. Philadelphia chromosome-negative chronic myeloproliferative disease. *Am J Clin Pathol* 2009;132:261–280.
23. Randi ML, Putti MC, Scapin M, et al. Pediatric patients with essential thrombocythemia are mostly polyclonal and V617F/JAK2 negative. *Blood* 2006;108:3600–3602.
24. Campbell PJ, Scott LM, Buck G, et al. Definition of subtypes of essential thrombocythemia and relation to polycythemia vera based on JAK2 V617F mutation status: A prospective study. *Lancet* 2005;366:1945–1953.
25. Cario H, Schwarz K, Herter JM, et al. Clinical and molecular characterisation of a prospectively collected cohort of children and adolescents with polycythemia vera. *Br J Haematol* 2008;142:622–626.
26. Tefferi A. Novel mutations and their functional and clinical relevance in myeloproliferative neoplasms: JAK2, MPL, TET2, ASXL1, CBL, IDH and IKZF1. *Leukemia* 2010;24:1128–1138.
27. Teofili L, Larocca LM. Advances in understanding the pathogenesis of familial thrombocythemia. *Br J Haematol* 2011;152:701–712.
28. Rives S, Pahl HL, Florensa L, et al. Molecular genetic analyses in familial and sporadic congenital primary erythrocytosis. *Haematologica* 2007;92:674–677.
29. Semenza GL. Involvement of oxygen-sensing pathways in physiologic and pathologic erythropoiesis. *Blood* 2009;114:2015–2019.
30. Randi ML, Murgia A, Putti MC, et al. Low frequency of VHL gene mutations in young individuals with polycythemia and high serum erythropoietin. *Haematologica* 2005;90:689–691.
31. Percy MJ, Furlow PW, Beer PA, et al. A novel erythrocytosis-associated PHD2 mutation suggests the location of a HIF binding groove. *Blood* 2007;110:2193–2196.
32. Percy MJ, Furlow PW, Lucas GS, et al. A gain-of-function mutation in the HIF2A gene in familial erythrocytosis. *N Engl J Med* 2008;358:162–168.
33. Abdel-Wahab O, Manshour T, Patel J, et al. Genetic analysis of transforming events that convert chronic myeloproliferative neoplasms to leukemias. *Cancer Res* 2010;70:447–452.

## Acceptable HLA-mismatching in unrelated donor bone marrow transplantation for patients with acquired severe aplastic anemia

Hiroshi Yagasaki,<sup>1,2</sup> Seiji Kojima,<sup>2</sup> Hiromasa Yabe,<sup>3</sup> Koji Kato,<sup>4</sup> Hisato Kigasawa,<sup>5</sup> Hisashi Sakamaki,<sup>6</sup> Masahiro Tsuchida,<sup>7</sup> Shunichi Kato,<sup>3</sup> Takakazu Kawase,<sup>8</sup> Yasuo Morishima,<sup>9</sup> and Yoshihisa Kodera,<sup>10</sup> for The Japan Marrow Donor Program

<sup>1</sup>Department of Pediatrics, Nihon University School of Medicine, Tokyo, Japan; <sup>2</sup>Department of Pediatrics, Nagoya University Graduate School of Medicine, Nagoya, Japan; <sup>3</sup>Department of Cell Transplantation and Regenerative Medicine, Tokai University School of Medicine, Isehara, Japan; <sup>4</sup>Children's Medical Center, Japanese Red Cross Nagoya First Hospital, Nagoya, Japan; <sup>5</sup>Kanagawa Children's Hospital, Yokohama, Japan; <sup>6</sup>Department of Hematology, Tokyo Metropolitan Komagome Hospital, Tokyo, Japan; <sup>7</sup>Ibaragi Children's Hospital, Mito, Japan; <sup>8</sup>Division of Immunology, Aichi Cancer Center, Nagoya, Japan; <sup>9</sup>Department of Hematology and Cell Therapy, Aichi Cancer Center, Nagoya, Japan; and <sup>10</sup>Department of Promotion for Blood and Marrow Transplantation, Aichi Medical University School of Medicine, Nagakute, Japan

We retrospectively analyzed the effect of HLA mismatching (HLA-A, -B, -C, -DRB1, -DQB1) with molecular typing on transplantation outcome for 301 patients with acquired severe aplastic anemia (SAA) who received an unrelated BM transplant through the Japan Marrow Donor Program. Additional effect of HLA-DPB1 mismatching was analyzed for 10 of 10 or 9 of 10 HLA allele-matched pairs (n = 169). Of the 301 recipient/donor pairs, 101 (33.6%)

were completely matched at 10 of 10 alleles, 69 (23%) were mismatched at 1 allele, and 131 (43.5%) were mismatched at  $\geq 2$  alleles. Subjects were classified into 5 subgroups: complete match group (group I); single-allele mismatch group (groups II and III); multiple alleles restricted to HLA-C, -DRB1, and -DQB1 mismatch group (group IV); and others (group V). Multivariate analysis indicated that only HLA disparity of group V was a significant risk

factor for poor survival and grade II-IV acute GVHD. HLA-DPB1 mismatching was not associated with any clinical outcome. We recommend the use of an HLA 10 of 10 allele-matched unrelated donor. However, if such a donor is not available, any single-allele or multiple-allele (HLA-C, -DRB1, -DQB1) mismatched donor is acceptable as an unrelated donor for patients with severe aplastic anemia. (*Blood*. 2011;118(11):3186-3190)

### Introduction

BM transplantation from an unrelated donor (UBMT) is indicated as salvage therapy for patients with severe aplastic anemia (SAA) who fail to respond to immunosuppressive therapy. Early results of UBMT have not been encouraging because of a high incidence of graft failure and GVHD.<sup>1-3</sup> The Center for International Blood and Marrow Transplant Research (CIBMTR) reported the outcome of 232 patients with SAA who received an UBM transplant between 1988 and 1998.<sup>3</sup> The 5-year probabilities of overall survival (OS) were 39% and 36% after matched unrelated and mismatched unrelated donor transplantations, respectively. We previously reported the outcome of 154 patients with SAA who received an UBM transplant between 1993 and 2000 through the Japan Marrow Donor Program (JMDFP).<sup>4</sup> The 5-year OS rate was 56% in that study.

In several recent studies, the effect of HLA high-resolution matching on outcome of patients who received an UBM transplant has been elucidated.<sup>5-8</sup> However, results have been derived primarily from an analysis of patients with hematologic malignancies. Major obstacles for UBMT are different between patients with hematologic malignancies and patients with SAA. Relapse is a main cause of death for patients with hematologic malignancies, and GVL effect may result in decrease of relapse rate. In contrast, graft failure is the main problem, and GVHD is the only negative effect for patients with SAA. Therefore, optimal HLA matching may be different between these 2 populations. Algorithms for donor selection derived from an analysis of patients with hemato-

logic malignancies might not be useful for patients with SAA. However, a few studies have focused on the clinical significance of HLA-allele compatibility in patients with SAA.<sup>2,4,9,10</sup>

In a previous study, we analyzed the clinical significance of HLA allele mismatching in 142 patients with SAA, in whom data of high-resolution typing of HLA-A, -B, and -DRB1 were available.<sup>4</sup> Mismatching of HLA-A or -B alleles between donor and recipient was a strong risk factor for acute and chronic GVHD and OS, whereas mismatching of the HLA-DRB1 allele did not have a significant effect on patient outcomes. In the study from the National Marrow Donor Program, mismatching of HLA-DRB1 was the most crucial risk factor for OS.<sup>2</sup> These results indicate that better donor selection through high-resolution typing might result in improved outcome in patients with SAA who receive an UBM transplant. In fact, several recent studies showed a significantly improved outcome in patients with SAA who received an UBM transplant over time.<sup>11,12</sup> In particular, better HLA matching by high-resolution typing has been thought to contribute to these improvements.<sup>4,9-11</sup>

On the contrary, restricting BMT to donor-recipient pairs perfectly matched at high-resolution typing reduces the chance of undergoing UBMT for many patients. Therefore, strategies for selecting a partially HLA allele mismatched donor are required when a full matched donor cannot be identified. Here, we report a detailed analysis of outcome in 301 patients with SAA who were

Submitted April 22, 2011; accepted June 18, 2011. Prepublished online as *Blood* First Edition paper, July 14, 2011; DOI 10.1182/blood-2011-04-349316.

The publication costs of this article were defrayed in part by page charge payment. Therefore, and solely to indicate this fact, this article is hereby marked "advertisement" in accordance with 18 USC section 1734.

The online version of this article contains a data supplement.

© 2011 by The American Society of Hematology

typed for HLA-A, -B, -C, -DRB1, -DQB1, and -DPB1 by a molecular technique and underwent UBT through the JMDF.

## Methods

### Patients

From February 1993 to April 2005, 380 consecutive patients with acquired SAA received an UBT transplant through the JMDF. Patients with inherited AA, such as Fanconi anemia, and patients who received a BM transplant > 2 times were excluded. This study includes 301 patients in whom molecular analysis of HLA-A, -B, -C, DRB1, and -DQB1 were performed by DNA-based methods. HLA-DPB1 was analyzed in 299 of these patients. The previous study included 142 patients in whom molecular typing was performed only for HLA-A, -B, and -DRB1.

Characteristics of the 301 patients and donors are shown in Table 1. Briefly, patients (173 males and 128 females) were between birth and 64 years of age (median, 17 years of age). The median disease duration before BMT was 43 months (range, 4-436 months). All patients failed conventional immunosuppressive therapies and were considered candidates for UBT. All patients or their guardians gave informed consent for transplantation and submission of the data to the JMDF.

### Transplantation procedure

Characteristics of the transplantation procedures are also shown in Table 1. Patients underwent transplantations at individual centers following the local protocols for preconditioning regimens and GVHD prophylaxis. The various preconditioning regimens used by individual centers were classified into 5 categories: TBI or LFI + CY + ATG (n = 128), TBI or LFI + CY (n = 103), TBI or LFI + CY + Flu with or without ATG (n = 39), CY + Flu + ATG (n = 8), and others (n = 23). In 130 patients, CsA and MTX were used for prophylaxis against GVHD; 134 patients received FK instead of CsA. The remaining 35 patients received other GVHD prophylaxis. Ex vivo T-cell depletion was not used for any patient. The median number of infused nucleated marrow cells was  $3.1 \times 10^8$ /kg. One-half (n = 150) of the transplantations were performed before 2000, and 151 were done after 2001.

### HLA typing and definition of mismatching

HLA matching between patients and donors was based on HLA serotyping according to the standard technique. Partial HLA-A and -B alleles and complete HLA-DRB1 alleles were identified as confirmatory HLA typing during the coordination process, and HLA-A, -B, -C, -DQB1, and -DPB1 alleles were retrospectively reconfirmed or identified after transplantation. Molecular typing of HLA-A, -B, -C, -DQB1, -DRB1, and -DPB1 alleles was performed by the Luminex microbead method (Luminex 100 system) adjusted for the JMDF and in part by the sequencing-based typing method. Mismatching was defined as the presence of donor antigens or alleles not shared by the recipient (rejection vector) or the presence of recipient antigens or alleles not shared by the donor (GVHD vector).

### Definition of transplantation-related events

The day of engraftment was defined as the first day of 3 consecutive days on which neutrophil count exceeded  $0.5 \times 10^9$ /L. Patients who did not reach neutrophil counts  $> 0.5 \times 10^9$ /L for 3 consecutive days after transplantation were considered to have primary graft failure. Patients with initial engraftment in whom absolute neutrophil counts declined to  $< 0.5 \times 10^9$ /L subsequently were considered to have secondary graft failure. Acute GVHD was evaluated according to standard criteria in patients who achieved engraftment, and chronic GVHD was evaluated according to standard criteria in patients who achieved engraftment and survived > 100 days after transplantation.

### Data collection and statistical analysis

Transplantation data were collected with the use of standardized forms provided by the JMDF. Patient baseline information and follow-up reports

were submitted at 100 days and annually after transplantation. Analysis of patient outcome was performed with the date of last reported follow-up or date of death. Data were analyzed as of July 1, 2007.

Probability of OS and 95% confidence interval (95% CI) were estimated from the time of transplantation according to the Kaplan-Meier method. Cumulative incidence of neutrophil engraftment at day 42 was analyzed in the whole of patients by treating deaths until day 42 as a competing risk. Cumulative incidence of acute GVHD at day 100 was analyzed in patients who sustained engraftment by treating deaths until day 100 as a competing risk. Cumulative incidence of chronic GVHD at day 365 was analyzed in patients who sustained engraftment and survived longer than day 100 by treating deaths until day 365 as a competing risk. In univariate analysis, the log-rank test or Gray test was used to assess the significance of HLA allele mismatching on clinical outcomes. The Mann-Whitney *U* test was used to compare the median days of neutrophil engraftment. The chi-square test or Mann-Whitney *U* test was used to compare patient characteristics and transplantation procedures between the patient groups. All *P* values < .05 were considered statistically significant, whereas *P* values between .05 and .1 were considered as marginally significant.

Multivariate analyses were performed to assess the effect of HLA allele mismatching on the clinical outcome by Cox proportional hazard model (each mismatched group vs fully matched group; hazard risk = 1.0 as a reference group). Factors other than HLA mismatching included in the models were patient age, patient sex, donor age, donor sex, disease duration before BMT, infused cell dose, matching of ABO blood type, GVHD prophylaxis, and preconditioning regimens.

## Results

### HLA matching by DNA typing

Of the 301 recipient/donor pairs, 101 pairs (33%) were completely matched at HLA-A, -B, -C, -DRB1, and -DQB1 allele; 69 pairs (23%) were mismatched at 1 HLA allele; 59 pairs (20%) were mismatched at 2 HLA alleles; and 72 pairs (24%) were mismatched at  $\geq 3$  alleles (Table 2). The number and frequency of 1-allele and 2-allele mismatches in either GVHD or rejection vector or both vectors in each HLA allele were 55 (18.3%) and 7 (2.3%) in HLA-A allele, 32 (10.6%) and 2 (0.7%) in HLA-B allele, 130 (43.2%) and 10 (3.3%) in HLA-C allele, 68 (22.6%) and 5 (1.7%) in HLA-DRB1 allele, 80 (26.6%) and 13 (4.3%) in HLA-DQB1 allele, and 179 (59.5%) and 44 (14.6%) in HLA-DPB1 allele, respectively. Because the frequency of mismatching was too high at the DPB1 allele, analysis of DPB1 mismatching was separated from that of other alleles. In addition, because the number of single-allele mismatched pairs of HLA-A, -B, -C, -DRB1, and -DQB1 were too small for separate analyses, HLA-A and -B were grouped into the mismatch of the HLA-A or HLA-B allele (A/B) and HLA-DRB1 and -DQB1 into the mismatch of the HLA-DRB1 or HLA-DQB1 allele (DRB1/DQB1), respectively.

### Survival

Of the 301 patients, 202 are alive at the time of analysis with an observation time from 3 to 128 months (median, 44 months) after transplantation. Five-year OS was 66.3% (95% CI, 60.7%-72.5%) in the whole population (supplemental Figure 1, available on the *Blood* Web site; see the Supplemental Materials link at the top of the online article). Subgroup analyses were performed in 8 main subgroups (> 15 recipients) as follows: (1) complete match group (n = 101), (2) single locus (A/B) mismatch group (n = 20), (3) single (C) mismatch group (n = 42), (4) 2 loci (A/B + C) mismatch group (n = 20), (5) 2 loci (DRB1/DQB1) mismatch group (n = 19), (6) 3 loci (A/B + C) mismatch group (n = 15), (7) 3 loci (C + DRB1/DQB1) mismatch group (n = 29), and

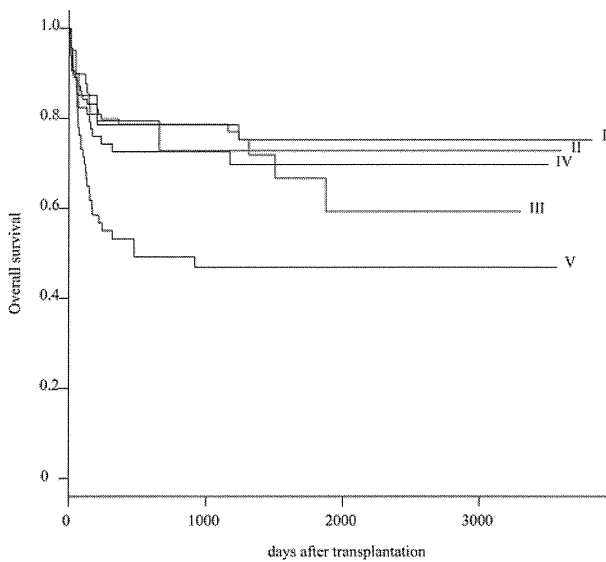


Figure 1. Kaplan-Meier estimates of OS in 5 HLA groups.

(8) 3 loci (A/B + C + DRB1/DQB1) mismatch group (n = 21). OS was significantly worse in the following groups than in the complete match group (75.2%): 2 loci (A/B + C) mismatch group (49.0%;  $P = .022$ ),  $\geq 3$  loci (A/B + C) mismatch group (40.0%;  $P = .002$ ), and A/B + C + DRB1/DQB1 mismatch group (56.1%;  $P = .031$ ; supplemental Table 1).

On the basis of these primary results, 301 patients were reclassified into 5 subgroups: HLA complete match group (group I; n = 101), single-allele (A/B) mismatch group (group II; n = 20), single-allele (C or DRB1/DQB1) mismatch group (group III; n = 49), multiple-allele (restricted to C or DRB1/DQB1) mismatch group (group IV; n = 68), and others (group V; n = 63). The probability of OS at 5 years was 75.2% (95% CI, 84.8%-66.7%) in group I, 72.7% (95% CI, 96.7%-54.7%) in group II, 66.7% (95% CI, 85.1%-52.3%) in group III, 69.7% (95% CI, 82.6%-58.8%) in group IV, and 46.8% (95% CI, 61.7%-35.5%) in group V, respectively (Table 3; Figure 1). Survival rate was significantly inferior in group V than in group I ( $P = .003$ ).

To avoid or minimize the effect of other HLA alleles mismatching, the effect of HLA-DPB1 mismatching was evaluated in group I (n = 101) and groups II + III (n = 69), independently. HLA-DPB1 was matched in 51 recipient/donor pairs (30%) and mismatched in 118 pairs (70%). Patient characteristics and transplantation procedures were not different between HLA-DPB1 matched and mismatched groups (supplemental Table 2). The probability of OS at 5 years in group I was equivalent between the HLA-DPB1 matched group (74.4%; 95% CI, 93.2%-59.4%) and the HLA-DPB1 mismatched group (75.7%; 95% CI, 87.2%-65.8%;  $P = .894$ ; Table 4; Figure 2A). It was also equivalent in groups II + III (71.4%; 95% CI, 93.6%-54.5% in the HLA-DPB1 matched group and in the HLA-DPB1 mismatched group (67.1%; 95% CI, 85.6%-52.5%;  $P = .826$ ; Table 4; Figure 2B). Multivariate analysis identified significant unfavorable variables as follows: recipient age (0-10 years: relative risk [RR] = 1.0; 11-20 years: RR = 4.092,  $P = .002$ ; 21-40 years: RR = 3.970,  $P = .004$ ; > 41 years: RR = 5.241,  $P = .003$ ), conditioning regimen (Flu + CY + TBI/LFI  $\pm$  ATG: RR = 1.0; CY + TBI/LFI: RR = 4.074,  $P = .058$ ; others: RR = 6.895,  $P = .013$ ), HLA mismatching (group I: RR = 1.0; group V: RR = 1.967,  $P = .023$ ), donor sex (female: RR = 1.0; male: RR = 1.850,  $P = .016$ ), and GVHD prophylaxis (FK + MTX: RR = 1.0; other: RR = 1.754,  $P = .024$ ), blood type

(ABO match or minor mismatch: RR = 1.0; major mismatch or bidirection: RR = 1.948,  $P = .005$ ), and disease duration (< 7 years: RR = 1.0; > 7 years: RR = 1.540,  $P = .084$ ; Table 5).

### Engraftment

The cumulative incidence of neutrophil engraftment at day 42 was evaluated in 300 patients. It was 90.3% (95% CI, 93.7%-86.9%) in the whole population. Subgroup analyses showed that it was 93.0% (95% CI, 98.2%-87.8%) in group I, 90.0% (95% CI, 100%-74.6%) in group II, 89.8% (95% CI, 98.9%-80.7%) in group III, 92.6% (95% CI, 99.2%-86.0%) in group IV, and 84.1% (95% CI, 93.4%-74.8%) in group V ( $P = .185$ ; Table 3). The median time to engraftment was 17 days in group I; 18 days in groups II, III, and IV; and 19 days in group V. Engraftment was marginally delayed in group V compared with group I ( $P = .053$ ). Additional HLA-DPB1 mismatching did not affect the cumulative incidence of engraftment in the 10 of 10 and 9 of 10 matched groups, respectively (Table 4). In multivariate analysis, blood type (ABO match or

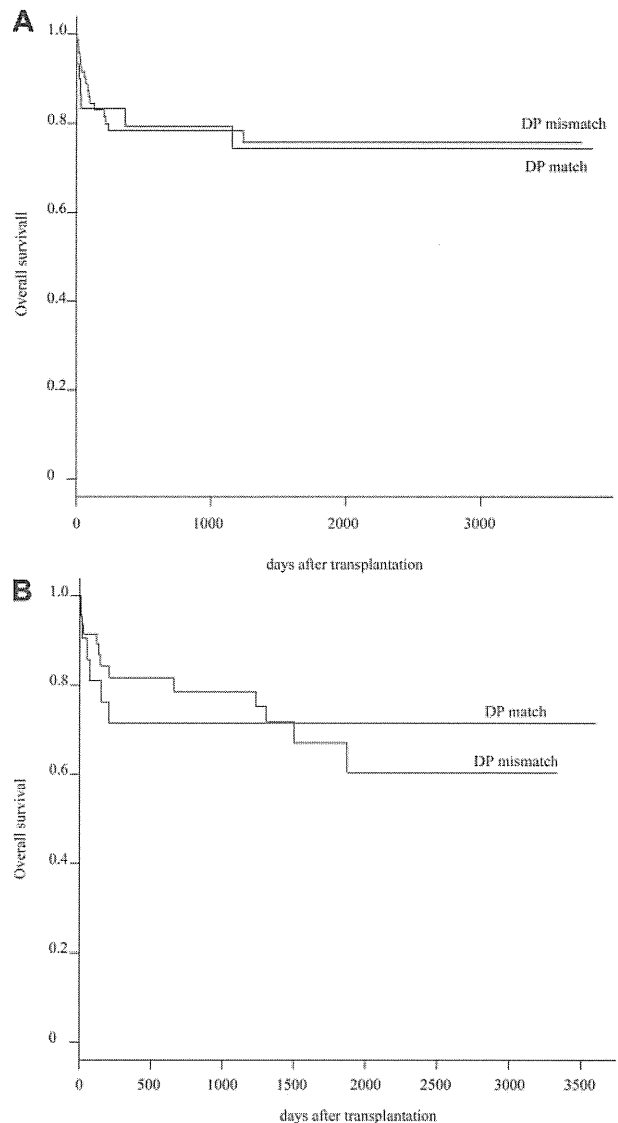
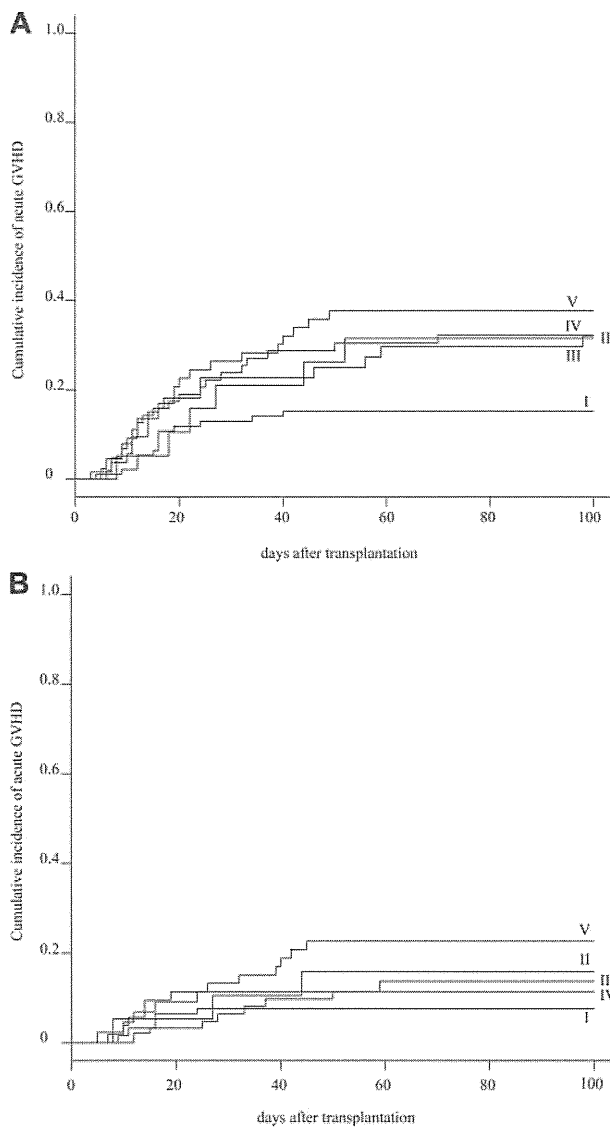


Figure 2. OS between HLA-DPB1 matched group and HLA-DPB1 mismatched group. (A) Difference of OS between HLA-DPB1 matched group and HLA-DPB1 mismatched group in 10 of 10 HLA allele matched pairs. (B) Difference of OS between HLA-DPB1 matched group and HLA-DPB1 mismatched group in 9 of 10 HLA allele matched pairs.



**Figure 3. Cumulative incidence of acute GVHD.** (A) Cumulative incidence of grade II-IV acute GVHD in 5 HLA groups. (B) Cumulative incidence of grade III-IV acute GVHD in 5 HLA groups.

minor mismatch: RR = 1.0; major mismatch or bidirection pair: RR = 5.102,  $P = .039$ ) and HLA mismatching (group I: RR = 1.0; group V: RR = 4.906,  $P = .035$ ) were significant risk factors for engraftment.

#### Acute GVHD

The cumulative incidence of acute GVHD at day 100 was evaluated in 272 patients. The cumulative incidence of grade II-IV and grade III-IV acute GVHD was 27.2% (95% CI, 32.5%-21.9%) and 12.9% (95% CI, 16.9%-8.9%) in the whole population, respectively (supplemental Figure 2). Subgroup analyses showed that the cumulative incidence of grades II-IV acute GVHD was statistically lower in group I (15.1%; 95% CI, 22.4%-7.8%) than in group V (37.7%; 95% CI, 50.9%-24.5%;  $P = .037$ ), and marginally lower than in group III (31.8%; 95% CI, 45.8%-17.8%) and group IV (31.7%; 95% CI, 43.3%-20.1%; Table 3; Figure 3A). Whereas the cumulative incidence of grade III-IV acute GVHD was not significantly different among 5 groups: 7.5% (95% CI, 24.6%-0%) in group I, 15.8% (95% CI, 32.7%-0%) in group II, 13.6% (95% CI, 23.9%-3.3%) in group III, 11.1% (95% CI,

18.9%-3.3%) in group IV, and 22.6% (95% CI, 34.0%-11.2%) in group V ( $P = .139$ ; Table 3; Figure 3B). Additional HLA-DPB1 mismatching evaluated in 155 patients did not affect the cumulative incidence of grade II-IV acute GVHD in the 10 of 10 and 9 of 10 matched groups, respectively (Table 4). Multivariate analysis showed that a significantly higher incidence of grade II-IV acute GVHD was associated with HLA mismatching (group I: RR = 1.0; group III: RR = 3.975,  $P = .002$ ; group IV: RR = 3.334,  $P = .004$ ; group V: RR = 3.665,  $P = .002$ ). Other significant risk factors were the preconditioning regimen (Flu + CY + TBI/LFI ± ATG: RR = 1.0; TBI/LFI + CY: RR = 5.224,  $P = .003$ ), and donor sex (female: RR = 1.0; male: RR = 1.844,  $P = .034$ ; supplemental Table 3).

#### Chronic GVHD

The cumulative incidence of chronic GVHD at day 365 was evaluated in 232 patients. It was 24.5% (95% CI, 30.3%-18.7%) in the whole population. Subgroup analyses showed that it was comparable among the 5 HLA groups: 19.8% (95% CI, 28.8%-10.8%) in group I, 26.3% (95% CI, 49.3%-3.3%) in group II, 28.2% (95% CI, 43.3%-13.1%) in group III, 26.9% (95% CI, 39.2%-14.6%) in group IV, and 27.3% (95% CI, 42.1%-12.5%) in group V ( $P = .922$ ; Table 3; supplemental Figure 3). HLA-DPB1 mismatching did not affect the cumulative incidence of chronic GVHD (Table 4).

#### Discussion

The survival rate in UMBT has increased substantially over the past 10 years in patients with SAA.<sup>8-15</sup> A 5-year survival rate of 90% has been reported in a small series of children.<sup>16,17</sup> A recent meta-analysis showed that detailed HLA-matching facilitated by DNA-based typing has contributed to the improved survival rate in patients with SAA who received an UMB transplant.<sup>18</sup> However, many patients with SAA who need hematopoietic stem cell transplantation do not have an HLA-complete matched donor. Our multivariate analysis indicated that among 4 HLA-mismatched groups, only HLA disparity of group V was a statistically significant unfavorable variable. We conclude that any type of HLA single-allele mismatch or multiple-allele mismatch within HLA-C and HLA class II (DRB1 or DQB1) is acceptable as an unrelated donor when an HLA complete match donor is unavailable.

We previously reported that HLA class I allele mismatching (HLA-A or -B) but not class II allele (HLA-DRB1) mismatching was a significant risk factor for survival when 6 alleles were analyzed.<sup>4</sup> HLA-A or -B mismatching pairs in the previous study were separated into 2 groups in the current study in which 10 alleles were analyzed. One group was a true single-allele mismatching pair of HLA-A or -B alleles (group II), and another was a multiple-allele mismatching pair of HLA-A or -B plus HLA-C and/or class II HLA alleles (group V). Because HLA-C and -DQB1 alleles were not typed, this type of multiple-allele mismatching might be mistaken as a single-allele mismatching pair, which was the reason for the inferior outcome of HLA-class I mismatching pairs in our previous study.

As the same in our previous study, mismatching of HLA-DRB1 did not provide a significant impact on clinical outcome. An HLA-DRB1 mismatching pair was also classified into a true single-allele mismatching of HLA-DRB1 (group III) and HLA-DRB1 plus HLA-C and/or HLA-DQB1 mismatching pairs (group IV). Interestingly, multiple mismatching of group IV was not



associated with increased mortality, which may explain why mismatching of HLA-DRB1 did not have a deleterious effect in the previous study.

The effect of HLA-DPB1 mismatching was also evaluated in HLA complete matched pairs (n = 101) and single-allele mismatched pairs (n = 69). The importance of DPB1 matching in the UBMT setting has been mainly discussed in patients with hematologic malignancies. Although results were controversial in early reports, recent studies support a significant effect of DPB1 mismatching on the incidence of acute GVHD, disease relapse, and OS.<sup>19-22</sup> In a large dataset of the International Histocompatibility Working Group, there was a statistically significant higher risk of both grade II-IV and grade III-IV acute GVHD.<sup>19</sup> The increased risk of acute GVHD was accompanied by a statistically significant decrease in disease relapse, probably because of the GVL effect, which offset the deleterious effect of acute GVHD. Survival rate was significantly better in DPB1-matched transplantations in patients with standard-risk leukemia but not in advanced leukemia. Conversely, in the HLA-mismatched group, there was a significant survival advantage in DPB1 mismatched pairs.

We expected that DPB1 matching might be beneficial for patients with AA who do not need the GVL effect. However, clinical outcomes, including incidence of acute GVHD, were not affected by DPB1 mismatching. HLA-DPB1 typing may not be essential to the donor selection algorithm for patients with SAA.

Indeed, HLA-DPB1 mismatching was observed in 74% of recipient/donor pairs, and it may be practically difficult to find HLA 12 of 12 matched donors.

In conclusion, this retrospective study confirms the importance of HLA matching between recipients and donors to improve the outcome of UBMT for patients with SAA patients. However, this study showed that only 33% of patients received transplants from an HLA 10 of 10 matched donor. The availability of unrelated hematopoietic stem cell transplants can be increased through the judicious selection of donors with HLA mismatches that do not substantially lower survival.

## Authorship

Contribution: H. Yagasaki analyzed the data and wrote the paper; S. Kojima designed the research and analyzed the data; and H. Yabe, K.K., H.K., H.S., M.T., S. Kato, T.K., Y.M., and Y.K performed and supervised the research.

Conflict-of-interest disclosure: The authors declare no competing financial interests.

Correspondence: Seiji Kojima, Department of Pediatrics, Nagoya University Graduate, School of Medicine, Tsurumai-cho 65, Showa-ku, Nagoya 466-8550, Japan; e-mail: kojimas@med.nagoya-u.ac.jp.

## References

- Hows J, Szydlo R, Anasetti C, Camitta B, Gajewski J, Gluckman E. Unrelated donor marrow transplants for severe acquired aplastic anemia. *Bone Marrow Transplant*. 1992;10(suppl 1):102-106.
- Deeg HJ, Seidel K, Casper J, et al. Marrow transplantation from unrelated donors for patients with severe aplastic anemia who have failed immunosuppressive therapy. *Biol Blood Marrow Transplant*. 1999;5(4):243-252.
- Passweg JR, Pérez WS, Eapen M, et al. Bone marrow transplants from mismatched related and unrelated donors for severe aplastic anemia. *Bone Marrow Transplant*. 2006;37(7):641-649.
- Kojima S, Matsuyama T, Kato S, et al. Outcome of 154 patients with severe aplastic anemia who received transplants from unrelated donors: the Japan Marrow Donor Program. *Blood*. 2002;100(3):799-803.
- Flomenberg N, Baxter-Lowe LA, Confer D, et al. Impact of HLA class I and class II high-resolution matching on outcomes of unrelated donor bone marrow transplantation: HLA-C mismatching is associated with a strong adverse effect on transplantation outcome. *Blood*. 2004;104(7):1923-1930.
- Morishima Y, Sasazuki T, Inoko H, et al. The clinical significance of human leukocyte antigen (HLA) allele compatibility in patients receiving a marrow transplant from serologically HLA-A, HLA-B, and HLA-DR matched unrelated donors. *Blood*. 2002;99(11):4200-4206.
- Morishima Y, Yabe T, Matsuo K, et al. Effects of HLA allele and killer immunoglobulin-like receptor ligand matching on clinical outcome in leukemia patients undergoing transplantation with T-cell-replete marrow from an unrelated donor. *Biol Blood Marrow Transplant*. 2007;13(3):315-328.
- Lee SJ, Klein J, Haagenson M, Baxter-Lowe LA, et al. High-resolution donor-recipient HLA matching contributes to the success of unrelated donor marrow transplantation. *Blood*. 2007;110(13):4576-4583.
- Kim SY, Lee JW, Lim J, et al. Unrelated donor bone marrow transplants for severe aplastic anemia with conditioning using total body irradiation and cyclophosphamide. *Biol Blood Marrow Transplant*. 2007;13(7):863-867.
- Perez-Albuerne ED, Eapen M, Klein J, et al. Outcome of unrelated donor stem cell transplantation for children with severe aplastic anemia. *Br J Haematol*. 2008;141(2):216-223.
- Maury S, Balere-Appert ML, Chir Z, et al. Unrelated stem cell transplantation for severe acquired aplastic anemia: improved outcome in the era of high-resolution HLA matching between donor and recipient. *Haematologica*. 2007;92(5):589-96.
- Viollier R, Socie G, Tichelli A, et al. Recent improvement in outcome of unrelated donor transplantation for aplastic anemia. *Bone Marrow Transplant*. 2008;41(1):45-50.
- Bacigalupo A, Locatelli F, Lanino E, et al. Fludarabine, cyclophosphamide and anti-thymocyte globulin for alternative donor transplants in acquired severe aplastic anemia: a report from the EBMT-SAA Working Party. *Bone Marrow Transplant*. 2005;36(11):947-950.
- Deeg HJ, O'Donnell M, Tolar J, et al. Optimization of conditioning for marrow transplantation from unrelated donors for patients with aplastic anemia after failure of immunosuppressive therapy. *Blood*. 2006;108(5):1485-1491.
- Lee JW, Cho BS, Lee SE, et al. The outcome of unrelated hematopoietic stem cell transplants with total body irradiation (800 cGy) and cyclophosphamide (120 mg/kg) in adult patients with acquired severe aplastic anemia. *Biol Blood Marrow Transplant*. 2011;17(1):101-108.
- Yagasaki H, Takahashi Y, Hama A, et al. Comparison of matched-sibling donor BMT and unrelated donor BMT in children and adolescent with acquired severe aplastic anemia. *Bone Marrow Transplant*. 2010;45(10):1508-1513.
- Kennedy-Nasser AA, Leung KS, Mahajan A, et al. Comparable outcomes of matched-related and alternative donor stem cell transplantation for pediatric severe aplastic anemia. *Biol Blood Marrow Transplant*. 2006;12(12):1277-1284.
- Peinemann F, Grouven U, Kröger N, Pittler M, Zschorlich B, Lange S. Unrelated donor stem cell transplantation in acquired severe aplastic anemia: a systematic review. *Haematologica*. 2009;94(12):1732-1742.
- Shaw BE, Gooley TA, Malkki M, et al. The importance of HLA-DPB1 in unrelated donor hematopoietic cell transplantation. *Blood*. 2007;110(13):4560-4566.
- Kawase T, Matsuo K, Kashiwase K, et al. HLA mismatch combinations associated with decreased risk of relapse: implications for the molecular mechanism. *Blood*. 2009;113(12):2851-2855.
- Crocchiolo R, Zino E, Vago L, et al. Nonpermissive HLA-DPB1 disparity is a significant independent risk factor for mortality after unrelated hematopoietic stem cell transplantation. *Blood*. 2009;114(7):1437-1444.
- Shaw BE, Mayor NP, Russell NH, et al. Diverging effects of HLA-DPB1 matching status on outcome following unrelated donor transplantation depending on disease stage and the degree of matching for other HLA alleles. *Leukemia*. 2010;24(1):58-65.

# Copy Number Variations Due to Large Genomic Deletion in X-Linked Chronic Granulomatous Disease

Takashi Arai<sup>1,7</sup>, Tsutomu Oh-ishi<sup>1,2</sup>, Hideaki Yamamoto<sup>1</sup>, Hiroyuki Nunoi<sup>3</sup>, Junji Kamizono<sup>4</sup>, Masahiko Uehara<sup>5</sup>, Takeo Kubota<sup>6</sup>, Takuya Sakurai<sup>7</sup>, Takako Kizaki<sup>7</sup>, Hideki Ohno<sup>7\*</sup>

**1** Department of Clinical Research, Saitama Children's Medical Center, Saitama, Japan, **2** Division of Infectious Disease, Saitama Children's Medical Center, Saitama, Japan, **3** Department of Pediatrics, Faculty of Medicine, University of Miyazaki, Miyazaki, Japan, **4** Department of Pediatrics, Kitakyusyu City Yahata Hospital, Kitakyusyu, Japan, **5** Department of Pediatrics, Health Insurance Hitoyoshi General Hospital, Hitoyoshi, Japan, **6** Department of Epigenetic Medicine, Interdisciplinary Graduate School of Medicine and Engineering, University of Yamanashi, Chuo, Japan, **7** Department of Molecular Predictive Medicine and Sport Science, Kyorin University, School of Medicine, Mitaka, Japan

## Abstract

Mutations in genes for any of the six subunits of NADPH oxidase cause chronic granulomatous disease (CGD), but almost 2/3 of CGD cases are caused by mutations in the X-linked *CYBB* gene, also known as NAD (P) H oxidase 2. Approximately 260 patients with CGD have been reported in Japan, of whom 92 were shown to have mutations of the *CYBB* gene and 16 to have chromosomal deletions. However, there has been very little detailed analysis of the range of the deletion or close understanding of the disease based on this. We therefore analyzed genomic rearrangements in X-linked CGD using array comparative genomic hybridization analysis, revealing the extent and the types of the deletion genes. The subjects were five Japanese X-linked CGD patients estimated to have large base deletions of 1 kb or more in the *CYBB* gene (four male patients, one female patient) and the mothers of four of those patients. The five Japanese patients were found to range from a patient exhibiting deletions only of the *CYBB* gene to a female patient exhibiting an extensive DNA deletion and the DMD and CGD phenotype manifested. Of the other three patients, two exhibited *CYBB*, *XK*, and *DYNLT3* gene deletions. The remaining patient exhibited both a deletion encompassing DNA subsequent to the *CYBB* region following intron 2 and the *DYNLT3* gene and a complex copy number variation involving the insertion of an inverted duplication of a region from the centromere side of *DYNLT3* into the deleted region.

**Citation:** Arai T, Oh-ishi T, Yamamoto H, Nunoi H, Kamizono J, et al. (2012) Copy Number Variations Due to Large Genomic Deletion in X-Linked Chronic Granulomatous Disease. PLoS ONE 7(2): e27782. doi:10.1371/journal.pone.0027782

**Editor:** Sunil K. Ahuja, South Texas Veterans Health Care System and University Health Science Center San Antonio, United States of America

**Received:** July 13, 2011; **Accepted:** October 25, 2011; **Published:** February 27, 2012

**Copyright:** © 2012 Arai et al. This is an open-access article distributed under the terms of the Creative Commons Attribution License, which permits unrestricted use, distribution, and reproduction in any medium, provided the original author and source are credited.

**Funding:** This work was partially supported by Grants-in-Aid for Specific Project Research from the Ministry of Education, Culture, Sport, Science and Technology of Japan. The funders had no role in study design, data collection and analysis, decision to publish, or preparation of the manuscript. No additional external funding received for this study.

**Competing Interests:** The authors have declared that no competing interests exist.

\* E-mail: ohnoh2o@kyorin-u.ac.jp

## Introduction

Chronic granulomatous disease (CGD [OMIM 306400]) is caused by a reduced nicotinamide adenine dinucleotide phosphate (NADPH) oxidase complex deficiency and is a primary immunodeficiency that impairs the bacteria-killing ability of phagocytes in the innate immune system and occurs with an incidence of 1 in 200,000 births per year [1]. The NADPH oxidase complex is localized in the cell membrane and is composed of heterodimeric membrane-bound flavocytochrome subunits formed from *gp91<sup>phox</sup>* (phox for phagocyte oxidase [OMIM 300481]) and *p22<sup>phox</sup>* (OMIM 233690) and cytoplasmic subunits formed from *p47<sup>phox</sup>* (OMIM 233700), *p67<sup>phox</sup>* (OMIM 233710), *p40<sup>phox</sup>*, and *Rac2* (OMIM 602049). Reactive oxygen species (ROS) required to kill microorganisms, such as superoxide anions (O<sub>2</sub><sup>•-</sup>) and hydrogen peroxide, are produced by the transfer of electrons from NADPH to oxygen molecules. In CGD, however, since the NADPH oxidase complex is defective or dysfunctional, it is not possible to kill microorganisms, although the leukocyte phagocytoses the microorganisms, and this leads to repeated infections by fungi and catalase-positive bacteria, such as *Staphylococcus*, *Pseudomonas*

*aeruginosa*, *Escherichia coli*, and *Klebsiella pneumoniae*, and frequently causes fatal granulomatous inflammation.

Mutations in genes for any of the six subunits of NADPH oxidase cause CGD, but almost 2/3 of CGD cases are caused by mutations in the X-linked *CYBB* gene, which codes for *gp91<sup>phox</sup>*. Other CGD patients all show autosomal recessive inheritance patterns. *CYBB* is located at Xp21.1 and is a 33.4 kb gene made up of 13 coding exons and a promoter region mainly expressed in phagocytes. Its mutations have been reported to include non-sense mutations, missense mutations, splice site mutations, duplications, deletions, and insertions [2]. In Japan, more than 260 patients with CGD have been reported [3]. Genetic analysis of the 92 patients with *CYBB* gene mutations was performed. Mutations similar to those in the above reports were found, but in five of the 16 cases exhibiting deletions, the deletion was estimated to be large at 1 kb or more. Quite recently, details have been revealed from two patients of five exhibiting contiguous gene syndrome (CGS) associated with deletions of the *XK* gene responsible for McLeod syndrome (OMIM 314850) and the ornithine transcarbamylase (*OTC*) gene responsible for OTC deficiency (OTCD [OMIM 311250]) [4].

However, it is often difficult to detect multiple exon deletions and multigene deletions with conventional PCR-SSCP analysis and DNA sequencing, hindering the precise search for gene duplications and the detection of heterozygous deletions and duplications in female carriers. In addition, it is technically difficult to use Southern blot analysis for high precision, extensive deletion searches. Because of this, the details of the types of genomic rearrangements including duplications and deletions (genomic copy-number losses and gains) and their ranges (sizes and boundaries) in X-linked CGD caused by mutations in the *CYBB* gene are largely unresolved.

Array comparative genomic hybridization (aCGH) is a method that has been successfully adapted to the detection of copy number variations (CNVs) in OTCD and Duchenne/Becker muscular dystrophy (DMD [MIM 310200]), has been confirmed to show high sensitivity compared with traditional methods currently available, and has been developing rapidly in recent years [5,6]. In the present study, we analyzed genomic rearrangements in Japanese X-linked CGD patients using aCGH analysis, revealing the extent and the types of the deletion genes.

## Results

### Search for the *CYBB* gene and *XK* gene by PCR

In patients 1, 3, and 4, neither exon 1 nor exon 13 of the *CYBB* gene was detected. In patient 2, exon 1 of the *CYBB* gene was detected, but exon 13 was not. In patient 5, both exon 1 and exon 13 of the *CYBB* gene were detected. A search for the *XK* gene was performed. Exon 1 of the *XK* gene was detected in patients 1, 2, and 5, but not in patient 3 or 4. In the healthy controls, on the other hand, exons 1 and 13 of the *CYBB* gene and exon 1 of the *XK* gene were clearly detected (Figure 1). These results suggested that while genes are present upstream of the *XK* gene in patient 1, at the very least, all *CYBB* gene exons are deleted, and that extensive deletions encompassing the *CYBB* gene and *XK* gene are

exhibited in patients 3 and 4. Deletion of *CYBB* exon 13 and the centromere side was suspected in patient 2. Patient 5 exhibited a similar gene amplification pattern to the healthy controls, and no obvious abnormality was observed.

### Deletion search by aCGH

The results of the search for CNVs by aCGH are summarized in Table 1. Deletions were observed in all five patients. Patient 1 showed the smallest deletion of the five patients at 58.7 kb, starting upstream of the *CYBB* gene and including all the exons of the 33.4 kb *CYBB* gene (Figure 2). Patient 2 was shown to exhibit a complex CNV involving a deletion of 84.4 kb encompassing the region downstream of exon 1 of the *CYBB* gene and the *DYNLT3* gene base sequence and a base sequence duplication of 91.9 kb adjacent to the centromere side of the deletion region (Figure 3). Patients 3 and 4 showed large deletions of 0.59 Mb and 1.94 Mb, respectively, encompassing the *XK* and *CYBB* genes and the *DYNLT3* gene (OMIM 300302), the function of which is not yet clear (Figure 4). Patient 5 showed an extensive deletion (5.71 Mb), exhibiting deletion of exons 1 to 42 of the 79 exons making up the *DMD* gene in addition to deletion of the *DYNLT3* gene, *CYBB* gene, and *XK* gene (Figure 5). aCGH of the mother of patient 5 also revealed a deletion of the same extent as in patient 5. The size of the genomic DNA deletions is half of that in the healthy female controls. Specifically, this shows that patient 5 has a deletion in the maternally inherited X-chromosome. With the exception of the mother of patient 4, who could not be tested, the mothers of the other four patients all had the same CNVs as their children, and the CNVs in patient 4 were heritable, rather than de novo (Table 1).

### Breakpoint analysis

A common TA base sequence was observed at breakpoints in patient 1 and the deletion of chrX:g.37364030\_37428980del64950 (UCSC hg17 May 2004) was observed (Figure 2). The breakpoint at

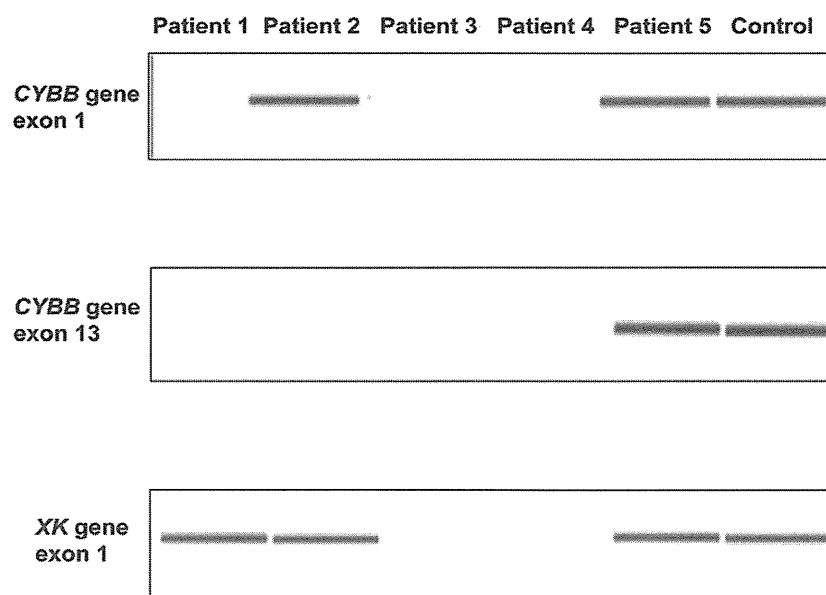


**Figure 1. PCR Amplification Results for Exons 1 and 13 of the Chronic Granulomatous Disease Gene *CYBB* and Exon 1 of the McLeod Syndrome Gene *XK* Region.** The analysis used the Agilent 2100 Bioanalyzer. Patients 1 to 5 were juvenile patients with chronic granulomatous disease, and genes from normal boys were amplified as a control. *CYBB* exon 1 was detected only from patients 2 and 5, and *CYBB* exon 13 only from patient 5. In addition, *XK* exon 1 was detected in patients 1, 2 and 5. doi:10.1371/journal.pone.0027782.g001

**Table 1.** The Results of aCGH Analysis of the Length of the Gene-Deleted Region and Disease Genes.

Patient	Sex	Deletion gene	Genotype (UCSC hg17 May 2004)	aCGH Deletions size (kb)	mother
1	M	<i>CYBB</i>	chrX:g.(37367763_37367821)_(37426362_37426421) del	58.7	carrier
2	M	<i>CYBB, DYNLT3</i>	chrX:g.(37402945_37403004)_(37487331_37487390) del	84.4	carrier
			chrX:g.(37514480_37514539)_(37606312_37606370) dup	91.9	
3	M	<i>XK, CYBB, DYNLT3</i>	chrX:g.(37128233_37128292)_(37722014_37722073) del	593.8	carrier
4	M	<i>XK, CYBB, DYNLT3</i>	chrX:g.(35599031_35599090)_(37543467_37543526) del	1944.5	-
5	F	<i>DMD, XK, CYBB, DYNLT3</i>	chrX:g.(32167387_32167446)_(37878746_37878805) del	5711.4	carrier

CYBB, cytochrome b-245, beta polypeptide; XK, X-linked Kx blood group gene; DMD, Duchenne muscular dystrophy gene; DYNLT3, dynein, light chain, Tctex-type3. doi:10.1371/journal.pone.0027782.t001

the telomere side in patient 2 was shown by DNA walking analysis to be chrX:g.37398670 in intron 2 of the *CYBB* gene (Figure 3). The base sequence detected at the breakpoint was 5'-AGGTAT|GTGAGCTGCCAC----3' (| denotes the breakpoint). A search using NCBI Blast Human Sequences showed that this base sequence corresponded to a sequence inversion observed from chrX:g.37612397 on the telomere side of the complementary strand. On the other hand, a search in the neighborhood of chrX:g.37612392, thought to be the breakpoint on the centromere side, found the normal 5'-GTGGCAGCTCAC|ATACCTAATCTGGACAGC----3' chromosomal base sequence. Because of this, it is thought that a 91.9 kb base sequence duplication as well as the deletion of an 84.4 kb base sequence shown by the results including aCGH analysis occurred in patient 3, and that since the duplicate centromere side end had the sequence 5'-AGGTAT-3' on the complementary strand, one of the duplicate strands must have inverted and recombined with the common 5'-AGGTAT-3' sequence at the telomere side of the 5' breakpoint of the 84.4 kb deletion. However, although the base sequence of the binding region thought to be present between the duplicate strands was investigated by the step-by-step PCR method and DNA walking analysis, it is as yet unclear.

### Investigation of skewed lyonization by methylation specific PCR

The analysis was conducted using peripheral blood mononuclear cells (PBMCs) from patient 5 and her mother. An abnormal (with deletion) X-chromosome from the mother (X1: 186 bp allele) and a normal X-chromosome from the father (X2: 195 bp allele) had been inherited. In the patient, a markedly skewed inactivation pattern was observed in which X-chromosomes from which genes had been deleted were activated and X-chromosomes with normal gene alleles were inactivated (Figure 6).

### Discussion

The aCGH analysis showed gene deletions of various sizes ranging from 58.7 kb to 5.71 Mb. In patient 1, only the *CYBB* gene was deleted, whereas CGS associated with simultaneous deletions of adjacent genes occurred in the other patients.

In patients 1 and 2, precise breakpoints were analyzed by direct sequencing methods after amplification with PCR and DNA walking. Analysis of four patients including two patients<sup>4</sup> previously reported by us found two cases in which all genes within the breakpoints were deleted and one case each of complex

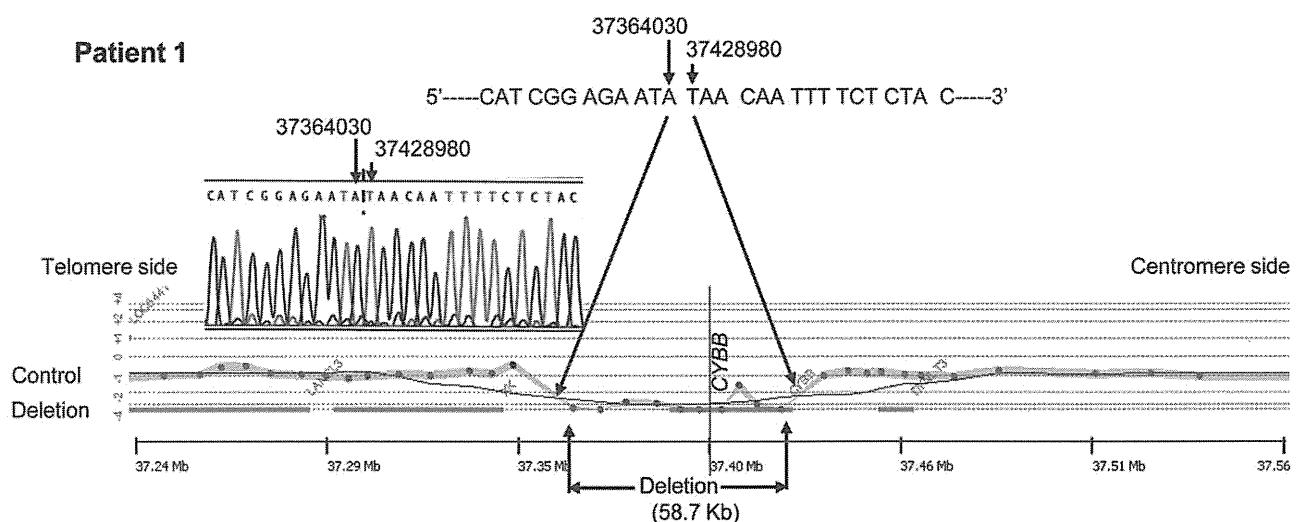


**Figure 2.** The Results of aCGH and Direct Sequence Analysis Spanning the Deletion Breakpoints in Patient 1. A female's DNA was used for the control DNA. aCGH analysis showed the deletion region to be 58.7 kb and direct sequencing after amplification by PCR showed that genes had been deleted from 37364030 to 37428980 (UCSC hg17 May,2004) and both breakpoints were bound.

doi:10.1371/journal.pone.0027782.g002

## Patient 2

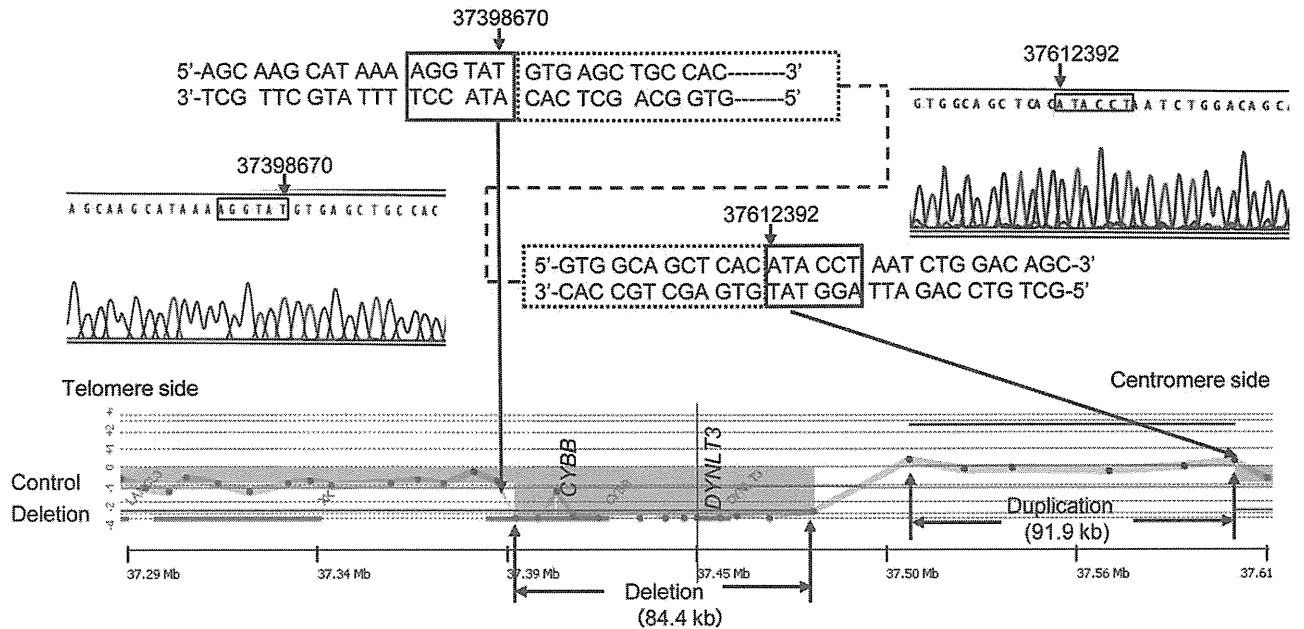
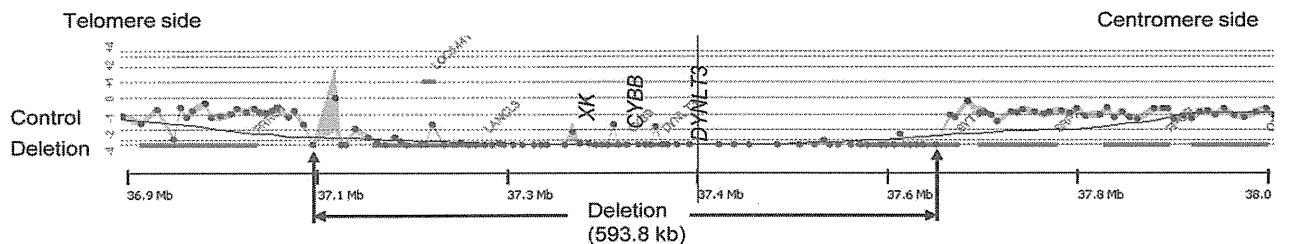


**Figure 3. The Results of aCGH and Direct Sequence Analysis Spanning the Deletion Breakpoints in Patient 2.** A female's DNA was used for the control. According to aCGH, the deletion site was 84.4 kbp and the duplication site 91.9 kb. According to the DNA walking analysis by PCR, a breakpoint was located at 37398670 of *CYBB* intron 2. Furthermore, six bases of the gene at 37612392 (UCSC hg17 May.2004) of ATACCT were bound inverted at the breakpoint, and complex structural abnormalities showing gene deletions on the inner side and duplication of the inverted part were observed.

doi:10.1371/journal.pone.0027782.g003

## Patient 3



## Patient 4

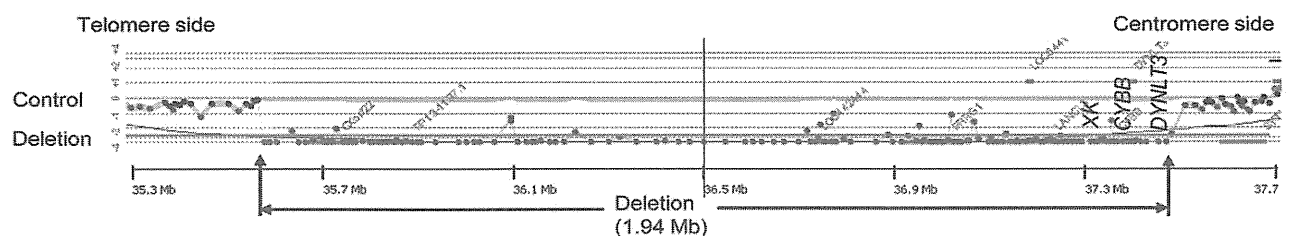


**Figure 4. The Results of aCGH Analysis Spanning the Deletion Breakpoints in Patients 3 and 4.** A female's DNA was used for the control DNA for patient 3, and a male's for patient 4. These male infants suffered deletions of three genes: the chronic granulomatous disease gene (*CYBB*), the McLeod syndrome gene (*XK*), and *DYNLT3*. The gene deletions in each patient were found to be 0.59 Mb and 1.94 Mb, respectively.

doi:10.1371/journal.pone.0027782.g004

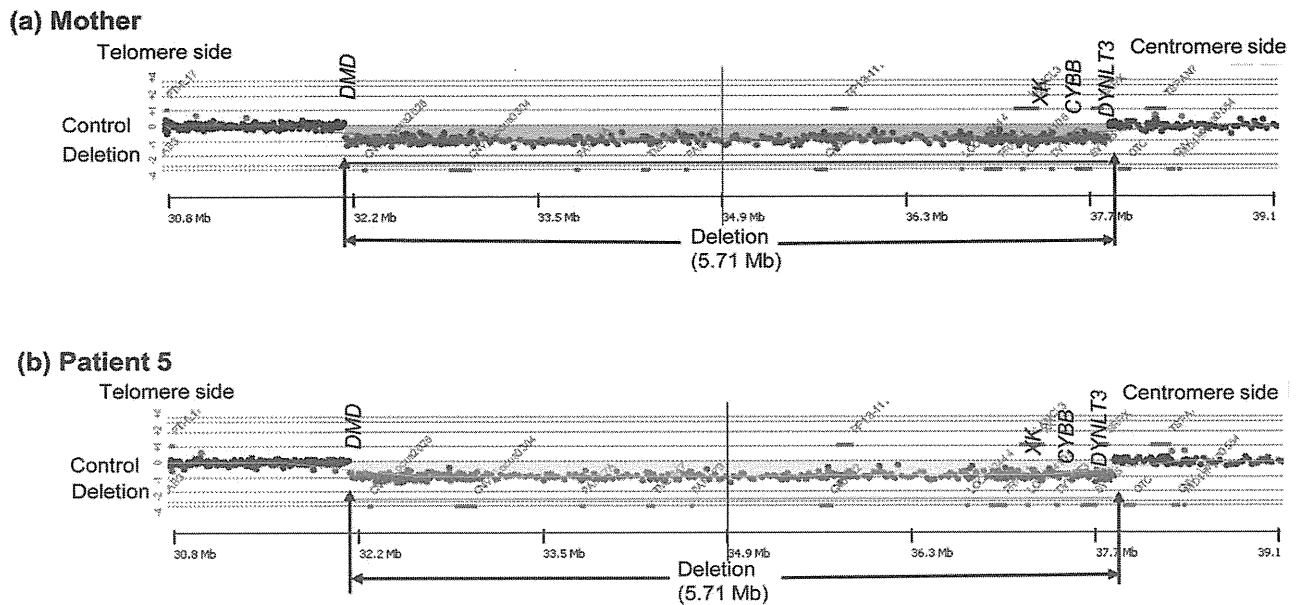


**Figure 5. The Results of aCGH Analysis Spanning the Deletion Breakpoints in Mother and Patient 5.** A female's DNA was used for the control DNA. This case involved deletions of four genes, the chronic granulomatous disease gene (*CYBB*), the Duchenne muscular dystrophy gene (*DMD*), the McLeod syndrome gene (*XK*), and *DYNLT3*. The gene deletion region was about 5.71 Mb and encompassed an area from *CYBB* to the greater part of the *DMD* (b). A similar gene deletion was also observed in the mother (a).  
doi:10.1371/journal.pone.0027782.g005

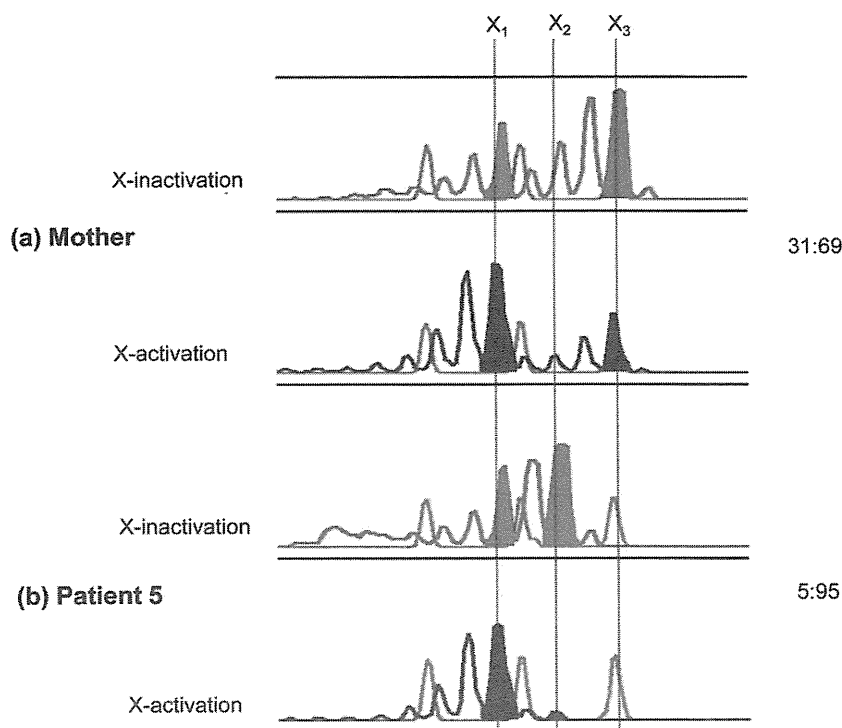


**Figure 6. The Results of an Analysis of X-Chromosome Inactivation and Activation Patterns in the Chronic Granulomatous Disease Sufferer Patient 5 and Her Mother.** The female infant had inherited an abnormal (with deletion) X-chromosome X<sub>1</sub> from the mother and a normal X-chromosome X<sub>2</sub> from the father. A random inactivation pattern of 69:31 was observed in the mother (carrier). In the female patient, however, a markedly skewed X-chromosome inactivation pattern of 95:5 (with activation of the X-chromosome with gene deletions transmitted from the mother and inactivation of the X-chromosome with the normal genes transmitted from the father) was observed.  
doi:10.1371/journal.pone.0027782.g006

structural abnormalities associated with gene insertions and further inversions in addition to deletions. The ends in four patients had no gene sequences expected to result in a common breakpoint.

Chromosomal deletions require a search over the entire range since variation in extent may produce false negatives by PCR and duplication of other regions may be involved. Conventionally, chromosome banding and fluorescence in situ hybridization (FISH) [7–9] have been used for analysis of chromosomal deletions, duplications, and translocations, but with chromosome banding, the detection limit is 1 Mb or more even in analyses with well-resolved prometaphase chromosomes. On the other hand, a combination of PCR and automated fluorescent DNA sequencing allows analysis of single base mutations on the chromosome and offers the highest resolution. However, the length of the deletion varies depending on the patient and for larger deletions, it is difficult to set primers. In addition, when no PCR products are generated, it is thought that nucleotide insertion into the deletion site or mutations in the base sequence at the primer binding site may have occurred. In recent years, aCGH has been developed and come into use as a method of analyzing CNVs on chromosomes. In principle, aCGH is a method of adhering a human gene-specific oligonucleotide probe to a glass slide and competitively hybridizing it with patient and control DNA, each labeled with different fluorochromes, and detecting deletions in the genome and amplification at a resolution of several kb by measuring the fluorescence. But while this method has high specificity and high resolution, it has the disadvantage including difficulty in identifying chromosomal translocations.

Deletions due to genomic mutations are often caused by tandem repeats and interspersed repeats. Interspersed repeats in particular include short direct repeats, interspersed repeat elements (e.g. Alu repeats), inverted repeats, low copy number long repeats, and active transposable elements and are prone to large scale deletions and duplications [10,11]. In patient 1, the entire *CYBB* gene within the breakpoints was deleted. The *CYBB* gene in patient 2 was found up to exon 2 and entirely deleted from exon 3. Moreover, it displayed a complex structure in which the breakpoint chrX:g.37398670 bound to the base sequence inverted from 37612392 and the region downstream of 37612392 (UCSC hg17 May. 2004) exhibited a successive existing base sequence. Alu sequences, which existed the most, were observed in the neighborhood of the ends, but were not directly involved in the breakpoints.

Patient 5 was female but was diagnosed with CGD, having a history of increased susceptibility to infection and confirmed as 46, X del (X) (p 21.1 p.21.2) on chromosome banding. aCGH showed that the mother was a carrier with an X-chromosome with the same deletion as the patient. The existence of skewed lyonization was investigated by analysis of X-chromosome inactivation on the basis of DNA methylation [12]. In the analysis of the patient and her mother, she had inherited an abnormal X-chromosome (X1: 186 bp allele) from her mother and a normal X-chromosome (X2: 195 bp allele) from her father. A markedly skewed inactivation pattern was observed in the patient, where the X-chromosome with deleted genes was activated and the X-chromosome having the normal genetic allele was inactivated (Fig. 6). In consideration of these results and of the measured percentage of gp91-positive cells in the patient's neutrophils (markedly low at about 5%) in addition to the notably decreased ability to produce ROS when measured by the NBT assay (as described later in the "Materials and Methods" section), the normal X-chromosome was thought to be inactivated in the majority of cells of this patient, which was believed to be a factor at the onset of the disease (a symptomatic carrier). Each cell expresses alleles from only one X-chromosome.

Reports on skewed lyonization include Bruton tyrosine kinase (BTK) deficiency (OMIM 300300) [13], DMD [14] and CGD [15–17], however, CGS associated with deletions to the same wide extent as in this patient has not been observed. Francke et al. [18] reported the case of a male infant in which CGD with extensive X-chromosome deletions was complicated by DMD, retinitis pigmentosa, and mental retardation. Here, we analyzed the case of a female infant who exhibited a similar phenotype with an extensive genomic deletion and revealed that the X-linked recessive disorder of women was caused by skewed lyonization.

While chromosomal deletions, inversions, and duplications occur singly or in combination, reciprocal recombinations due to translocations have been reported [19–21]. In patient 1, it was speculated that gene rearrangements due to non-homologous end-joining (NHEJ) showing the repeated sequence of only two bases (TA) at the ends of the deleted gene may have occurred (Figure 7.1a, 1b). Patient 2 had a complex structural abnormality, and it was hypothesized that this may have been caused by fork stalling and template switching (FoSTeS)/microhomology-mediated break-induced replication (MMBIR) [22,23]. In patient 2, a three base repeat sequence of AAT prone to cause changes in copy number or sequence swaps was observed in the original DNA strand that acts as a template for the lagging strand during DNA replication. This AAT is thought to bind to a complementary DNA sequence of TTA nearby on the same strand of DNA, forming a loop and inhibiting expansion of the replication fork (Figure 7.2a). Furthermore, releasing the leading strand with the free 3' end, AGGTAT, and binding to the complementary strand ATACCT of another replication fork, a leading strand 5'-AGGTATGTGAGC----3' was synthesized (Figure 7.2b). The gene synthesized on the leading strand is hypothesized to cause structural abnormalities leading to duplications and inversions of the DNA strand subsequent to the deleted DNA strand by a return to the lagging strand after the end of replication and the binding of the 5'----GCTCACATACCT-3' telomere side terminus with the normal gene to the 5'-AGGTATGTGAGC----3' centromere side terminus gene by DNA ligase (Figure 7.2c). As far as we could find, while a breakage-fusion-bridge cycle has been reported as a mechanism for large structural abnormalities causing deletions, inversions, and duplications during chromosome division [23], no cases of structural abnormalities occurring in the vicinity of the same gene have been observed.

## Materials and Methods

### Subjects

The subjects were five Japanese X-linked CGD patients estimated to have large base deletions of 1 kb or more in the *CYBB* gene (four male patients, one female patient) and the mothers of four of these patients. The four male patients were diagnosed as CGD on the basis of the past history with increased susceptibility to infection, and of deficiencies in ROS productivity by the nitroblue tetrazolium test (NBT) and the neutrophil chemiluminescence method. Two of the male patients exhibited reduced expression of erythrocyte Kell blood group antigen, acanthocytosis, and also high serum CPK activity. In the female infant patient, in addition to a history of increased susceptibility to infection at the age of 11 and a marked reduction in ROS productivity to around 5% of normal, chromosome banding showed 46, X, del (X)(p21.1p21.2), and CGD was clinically diagnosed.

### DNA isolation

All the patient samples in the present study were used with the approval of the Saitama Children's Medical Center Ethics

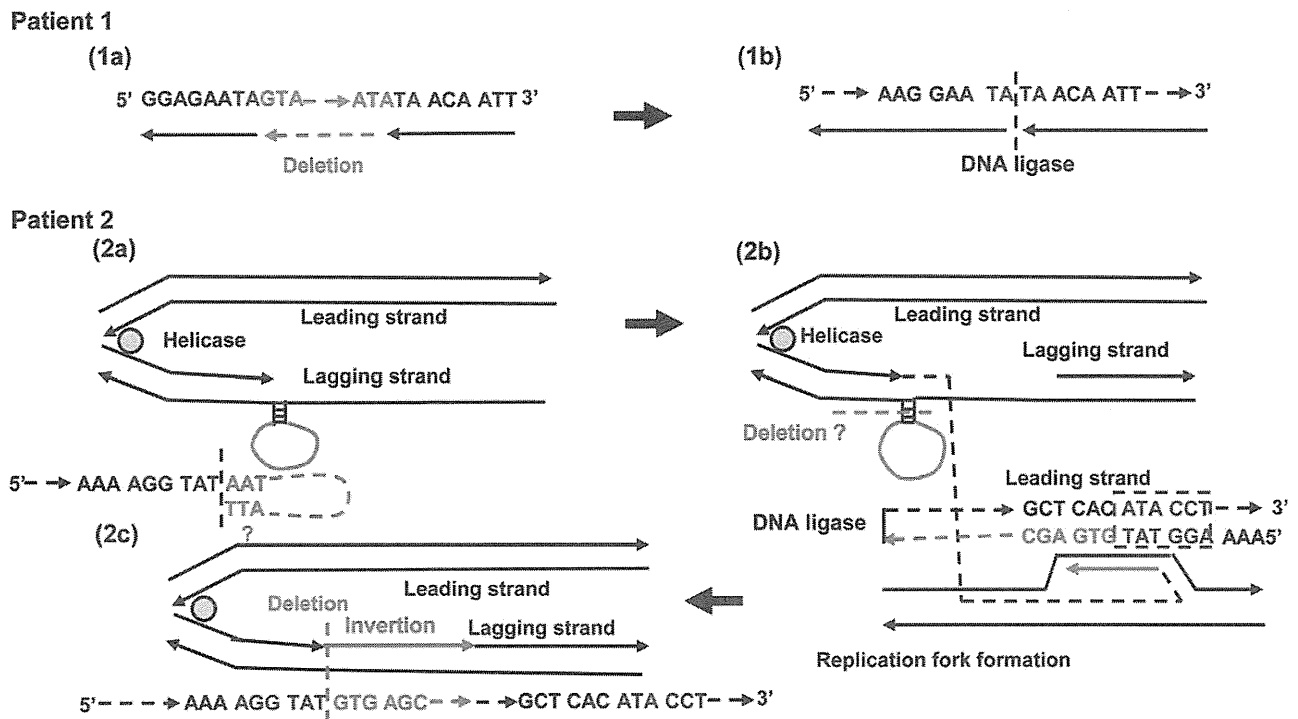


**Figure 7. Genomic Rearrangement Mechanisms.** For the gene deletions in patient 1, gene rearrangements exhibiting deletions due to non-homologous end-joining (NHEJ) were thought to have occurred, since repeated two base sequences of TA were observed at both ends of the gene (1a, 1b). In patient 2, it was hypothesized that rearrangement might have occurred through a mechanism involving a combination of fork stalling and template switching (FoSTeS)/microhomology-mediated break-induced replication (MMBIR). A three base repeat sequence of AAT prone to cause changes in copy number or sequence swaps was observed in a discontinuous end of the lagging strand during DNA replication. This formed a loop by binding to TTA on its complementary strand with replication slippage occurring (2a). At the discontinuous end, the lagging strand with the loop formed had a six base microhomology of AGGTAT and dissociated. The dissociated end subsequently bound to the ATACCT found at the duplication front of the leading strand. Synthesis and extension of the leading strand then occurred originating from the binding site (2b). The gene synthesized on the leading strand is hypothesized to cause structural abnormalities leading to duplications of the DNA strand subsequent to the DNA strand deletion by returning to the lagging strand after the end of duplication and the binding of the end that has finished duplication to the starting end of the normal gene on the lagging strand by DNA ligase (2c).  
 doi:10.1371/journal.pone.0027782.g007

Committee and after obtaining written informed consent, and the procedures were conducted to the principles expressed in the Declaration of Helsinki, 2008. Patient's parents provided written informed consent. DNA was extracted with a DNA Blood Mini Kit (Qiagen, Valencia, CA) after isolation of heparinized PBMCs.

#### PCR-band studies

*CYBB* gene and the adjacent X-linked Kx blood group-related *XK* gene were amplified by PCR and the detection of individual genes was attempted using the Agilent 2100 Bioanalyzer (Agilent Technologies, Santa Clara, CA) according to the manufacturer's instructions. The following primers were used for PCR: *CYBB* ex1: forward, 5'-AATGTGTTTTACCCAGCACG-3' and reverse, 5'-TGCTTTGGTCTATTTTATGTTCC-3'; *CYBB* ex13: forward, 5'-TAGACATCTCATCCCAAAGC-3' and reverse, 5'-TTA-TTTGAGCATTGGCAGC-3'; *XK* ex1: forward, 5'-TTTCCC-AAGATAGGACCC-3' and reverse, 5'-GTTGAACCACAA-GAACTGC-3'.

#### aCGH analysis

aCGH measurements used the Agilent Genomic DNA Labeling Kit (Agilent Technologies). In brief, 1 µg of each of the patient and control DNA (patients 1, 2, and 3: gender non-matched reference controls, patients 4 and 5: gender matched reference controls)

were digested with two restriction enzymes (AluI and RsaI; Life Technologies, Carlsbad, CA). Random-primed DNA labeling was performed according to the manufacturer's recommended protocol using Cy3-dUTP for patient DNA and Cy5-dUTP for control DNA. After reacting at 37°C for 2 hrs, labeled patient and control DNA were purified using DNA Microcon YM-3-filter units (Millipore, Billerica, MA), mixed, and human Cot-1 DNA (Life Technologies) and hybridization buffer (Agilent Technologies) were added. The mixed samples were applied to microarray slides (Human Genome CGH Microarray 244A, Agilent Technologies) and the microarray slides were hybridized in Agilent SureHyb chambers at 65°C for 40 hrs. After a second washing operation and microarray scanning (Agilent DNA microarray scanner and Agilent Scan Control Software), images were extracted using the Feature Extraction Software (version 9.5.3.1; Agilent Technologies) and imported into the Agilent CGH-Analytics V3.5.14 Software for analysis, and statistically significant CNVs were determined using the aberration detection module (ADM)-2 algorithm. For details of the statistical algorithm, the Agilent Technologies user's manual is available (<http://www.agilent.com/chem/goCGH>). Copy-number size was measured as the difference between the first and last probe position in the region deleted using the algorithm. The chromosome resolution of DNA variants with this method averaged 6.4 kb.



## Determining of breakpoints

Breakpoints were analyzed in patients 1 and 2. Deletions of telomeric and centromeric breakpoints revealed by the aCGH results of patient 1 were determined by the previously reported step-by-step PCR method [4] using the TAKARA Ex Taq (Takara Bio, Tokyo, Japan). Finally, after amplification by PCR with primers set to sandwich the telomeric and centromeric breakpoints, direct sequence analysis (ABI 310, Life Technologies) of the PCR product was performed. In patient 2, on the other hand, as shown in the results, it was not possible to find the breakpoints by the method described above. To determine the deletion breakpoints, a DNA walking analysis was conducted according to the manufacturer's instructions (DNA Walking Kit; Seegene, Rockville, MD). For patient 2, gene-specific primary 1stF 5'-GGAATCTACTGTGGAAATGC-3', 2ndF 5'-TGTTACAT-CATGCTGAAACTATG-3', 3rdF 5'-TCCCGCCAAAATATG-CAAC-3' and nested primers designed based on the base sequence near the telomeric breakpoint region were used for PCR amplification in combination with primary and nested PCR to Genome Walker Adaptors. To confirm the results, gene-specific

primers were designed to straddle the deletion breakpoints, and PCR products were amplified from genomic DNA. PCR products were analyzed by direct sequence analysis. Gene sequences obtained from the analysis were searched for genetic information using the NCBI's BLAST Human Sequences (<http://www.ncbi.nlm.nih.gov/genome/seq/BlastGen/BlastGen>). Androgen Receptor in the X-chromosome (the HUMARA region) of patient 5 was analyzed by methylation specific PCR and examined for skewed lyonization [12].

## Acknowledgments

We would like to thank all participating patients and staffs of collaborating institutes.

## Author Contributions

Conceived and designed the experiments: TA TO HO. Performed the experiments: TA HY. Analyzed the data: TA HY. Contributed reagents/materials/analysis tools: HN JK MU T. Kubota TS T. Kizaki. Wrote the paper: TA HO.

## References

- Johnston RB, Jr. (2001) Clinical aspects of chronic granulomatous disease. *Curr Opin Hematol* 8: 17–22.
- Roos D, Kuhns DB, Maddalena A, Roesler J, Lopez J, et al. (2010) Hematologically important mutations: X-linked chronic granulomatous disease (third update). *Blood Cells Mol Dis* 45: 246–265.
- Nunoi H (2007) Two breakthroughs in CGD studies. *Jap J Clin Immunol* 30: 1–10.
- Yamada M, Arai T, Oishi T, Hatana N, Kobayashi I, et al. (2010) Determination of the deletion breakpoints in two patients with contiguous gene syndrome encompassing CYBB gene. *Eur J Med Genet* 53: 383–388.
- del Gaudio D, Yang Y, Boggs BA, Schmitt ES, Lee JA, et al. (2008) Molecular diagnosis of Duchenne/Becker muscular dystrophy: enhanced detection of dystrophin gene rearrangements by oligonucleotide array-comparative genomic hybridization. *Hum Mutat* 29: 1100–1107.
- Shchelochkov OA, Li FY, Geraghty MT, Gallagher RC, Van Hove JL, et al. (2009) High-frequency detection of deletions and variable rearrangements at the ornithine transcarbamylase (OTC) locus by oligonucleotide array CGH. *Mol Genet Metab* 96: 97–105.
- Simon KC, Noack D, Rac J, Curnutte J, Sarraf S, et al. (2005) Long polymerase chain reaction-based fluorescence in situ hybridization analysis of female carriers of X-Linked chronic granulomatous disease deletions. *J Mol Diagn* 7: 183–186.
- Kabuki T, Kawai T, Kin Y, Joh K, Ohashi H, et al. (2003) A case of Williams syndrome with p47-phox-deficient chronic granulomatous disease. *Jap J Clin Immunol* 26: 299–303.
- Srouf M, Bejjani BA, Rorem EA, Hall N, Shaffer LG, et al. (2008) An instructive case of an 8-year-old boy with intellectual disability. *Semin Pediatr Neurol* 15: 154–155.
- Korenberg JR, Rykowski MC (1988) Human genome organization: Alu, LINES, and the molecular structure of metaphase chromosome bands. *Cell* 53: 391–400.
- Mazzarella R, Schlessinger D (1998) Pathological consequences of sequence duplications in the human genome. *Genome Res* 8: 1007–1021.
- Kubota T, Nonoyama S, Tonoki H, Masuno H, Imaizumi K, et al. (1999) A new assay for the analysis of X-chromosome inactivation based on methylation-specific PCR. *Hum Genet* 104: 49–55.
- Takada H, Kanegane H, Nomura A, Yamamoto K, et al. (2004) Female agammaglobulinemia due to the Bruton tyrosine kinase deficiency caused by extremely skewed X-chromosome inactivation. *Blood* 103: 185–187.
- Yoshida M, Yorifuji T, Mituyoshi I (1998) Skewed X inactivation in manifesting carriers of Duchenne muscular dystrophy. *Clin Genet* 52: 102–107.
- Gono T, Yazaki M, Agematsu K, Matsuda M, Yasui K, et al. (2008) Adult onset X-linked chronic granulomatous disease in a woman patient caused by a de novo mutation in paternal-origin CYBB gene and skewed inactivation of normal maternal X chromosome. *Inter Med* 47: 1053–1056.
- Lewis EM, Singla M, Sergeant S, Koty PP, McPhail LC (2008) X-linked chronic granulomatous disease secondary to skewed X chromosome and late presentation. *Clin Immunol* 129: 372–380.
- Anderson-Cohen M, Holland SM, Kuhns DB, Fleisher TA, Ding L, et al. (2003) Severe phenotype of chronic granulomatous disease presenting in a female with a de novo mutation in gp91-phox and a non familial, extremely skewed X chromosome inactivation. *Clin Immunol* 109: 308–317.
- Francke U, Ochs HD, De Martinville B, Giacalone J, Lindgren V, et al. (1985) Minor Xp21 chromosome deletion in a male associated with expression of duchenne muscular dystrophy, chronic granulomatous disease, retinitis pigmentosa, and McLeod syndrome. *Am J Hum Genet* 37: 250–267.
- Saunier S, Calado J, Benessy F, Silbermann F, Heilig R, et al. (2000) Characterization of the NPHP1 Locus: Mutation Mechanism Involved in Deletion in Familial Juvenile Nephronophthisis. *Am J Hum Genet* 66: 778–789.
- Shchelochkov OA, Cooper ML, Ou Z, Peacock S, Yatsenko SA, et al. (2008) Mosaicism for r(X) and del(X)del(X)(p11.23)dup(X) (p11.21p11.22) provides insight into the possible mechanism of rearrangement. *Mol Cytogenet* 1: 16.
- Bonaglia MC, Giorda R, Massagli A, Galluzzi R, et al. (2009) A familial inverted duplication/deletion of 2p25.1-25.3 provides new clues on the genesis of inverted duplications. *Eur J Hum Genet* 17: 179–186.
- Lee JA, Carvalho CM, Lupski JR (2007) A DNA replication mechanism for generating nonrecurrent rearrangements associated with genomic disorders. *Cell* 131: 1235–1247.
- Hastings PJ, Lupski JR, Rosenberg SM, Ira G (2009) Mechanisms of change in gene copy number. *Nat Rev Genet* 10: 551–564.

# Successful Treatment with Infliximab for Inflammatory Colitis in a Patient with X-linked Anhidrotic Ectodermal Dysplasia with Immunodeficiency

Tomoyuki Mizukami · Megumi Obara · Ryuta Nishikomori · Tomoki Kawai · Yoshihiro Tahara · Naoki Sameshima · Kousuke Marutsuka · Hiroshi Nakase · Nobuhiro Kimura · Toshio Heike · Hiroyuki Nunoi

Received: 23 July 2011 / Accepted: 15 September 2011 / Published online: 13 October 2011  
© Springer Science+Business Media, LLC 2011

**Abstract** X-linked anhidrotic ectodermal dysplasia with immunodeficiency (X-EDA-ID) is caused by hypomorphic mutations in the gene encoding nuclear factor- $\kappa$ B essential modulator protein (NEMO). Patients are susceptible to diverse pathogens due to insufficient cytokine and frequently show severe chronic colitis. An 11-year-old boy with X-EDA-ID was hospitalized with autoimmune symptoms and severe chronic colitis which had been refractory to immunosuppressive drugs. Since tumor necrosis factor (TNF)  $\alpha$  is responsible for the pathogenesis of NEMO colitis according to intestinal NEMO and additional TNFR1 knockout mice studies, and high levels of TNF $\alpha$ -producing mononuclear cells were detected in the patient due to the unexpected gene reversion mosaicism of NEMO, an anti-TNF $\alpha$  monoclonal antibody was administered

to ameliorate his abdominal symptoms. Repeated administrations improved his colonoscopic findings as well as his dry skin along with a reduction of TNF $\alpha$ -expressing T cells. These findings suggest TNF blockade therapy is of value for refractory NEMO colitis with gene reversion.

**Keywords** NEMO colitis · infliximab · gene reversion

## Introduction

X-linked anhidrotic ectodermal dysplasia with immunodeficiency (X-EDA-ID) is a rare inherited disease caused by hypomorphic mutations in the gene encoding nuclear factor- $\kappa$ B

**Electronic supplementary material** The online version of this article (doi:10.1007/s10875-011-9600-0) contains supplementary material, which is available to authorized users.

T. Mizukami · M. Obara · H. Nunoi (✉)  
Division of Pediatrics, Department of Reproductive and Developmental Medicine, Faculty of Medicine, University of Miyazaki,  
5200 Kihara, Kiyotake,  
Miyazaki 889-1692, Japan  
e-mail: h-nunoi@fc.miyazaki-u.ac.jp

T. Mizukami  
Kumamoto Saishunso National Hospital,  
Kumamoto, Japan

R. Nishikomori · T. Kawai · T. Heike  
Department of Pediatrics,  
Kyoto University Graduate School of Medicine,  
Kyoto, Japan

Y. Tahara  
Department of Gastroenterology and Hematology,  
Faculty of Medicine, University of Miyazaki,  
Miyazaki, Japan

N. Sameshima · K. Marutsuka  
Department of Pathophysiology, Faculty of Medicine,  
University of Miyazaki,  
Miyazaki, Japan

H. Nakase  
Department of Gastroenterology and Hepatology,  
Kyoto University Graduate School of Medicine,  
Kyoto, Japan

N. Kimura  
Division of Medical Oncology, Hematology and Infectious Disease, Department of Medicine, Fukuoka University,  
Fukuoka, Japan

(NF- $\kappa$ B) essential modulator (NEMO), which is the regulatory subunit of I $\kappa$ B kinase [1–3]. Mutations of NEMO can cause an impaired capacity to activate NF- $\kappa$ B, resulting in defects in ectodermal differentiation and innate and adaptive immunity [4, 5]. Affected patients generally show multiple developmental anomalies in ectodermal tissues such as sparse hair, hypodontia with conical teeth, and anhidrosis or hypohidrosis due to lack of sweat glands. These patients also suffer from severe life-threatening infections in various sites caused by Gram-positive or Gram-negative bacteria or mycobacteria. Immunological abnormalities are characterized by defects in the production of proinflammatory cytokines in response to lipopolysaccharide (LPS) stimulation, hypogammaglobulinemia, specific antibody deficiency, and natural killer cell dysfunction. Hematopoietic stem cell transplantation for X-EDA-ID has been employed as a curative treatment [6–10], but has sometimes resulted in engraftment failure.

NEMO colitis, which is inflammatory colitis associated with mutated NEMO protein [11], is found in one fifth of all X-EDA-ID patients [12] and is usually reported as inflammatory bowel disease (IBD), atypical colitis, or Behcet's disease [6, 11, 13]. The onset of inflammatory colitis occurs early in childhood and often causes failure to thrive [2, 5–7, 9, 11–13]. The age of onset of colitis in X-EDA-ID is earlier than that of Crohn's disease, ulcerative colitis, or chronic granulomatous disease [14]. Histological examination reveals active colitis with abundant neutrophilic infiltration, and the colitis usually improves with corticosteroids but not with antimicrobial agents [6, 11]. Susceptibility to colitis remains after hematopoietic stem cell transplantation [6, 9].

Recently, Nenci et al. demonstrated that mice lacking NEMO in intestinal epithelial cells developed spontaneous severe colitis [15]. However, an additional lack of tumor necrosis factor (TNF) receptor-1 in these mice inhibited intestinal inflammation. These interesting findings suggest that TNF $\alpha$  plays a role in the progression of NEMO colitis and that TNF blockade therapy would be a promising treatment.

We describe here an X-EDA-ID boy suffering from severe intractable colitis who improved dramatically following treatment with a chimeric anti-TNF $\alpha$  monoclonal antibody, infliximab. Infliximab administration reduced all symptoms relating to inflammatory colitis, not only frequent diarrhea and severe abdominal pain, but also inflammatory findings by colonoscopy. These effects have lasted for more than 2 years with regular administrations of infliximab.

## Methods

### Cell Preparation and Culture

Peripheral blood mononuclear cells (PBMCs) were isolated from peripheral blood from our X-EDA-ID patient and his

mother using Ficoll-Paque gradient centrifugation. PBMCs were suspended in RPMI 1640 medium (Sigma-Aldrich, USA) and non-adherent cells were used to obtain stimulated T cells. Adherent cells were cultured for 10 days with 500 U/mL granulocyte-macrophage colony-stimulating factor (GM-CSF) (Peprotech, USA) to induce monocyte proliferation. T cells were stimulated for 48 h with 1- $\mu$ g/mL phytohemagglutinin (PHA) (Seikagaku Kogyo, Japan) and then for 8 days with 10-U/mL recombinant human interleukin (IL)-2 (Genzyme Techne, USA).

### Cytokine Production Assay

PBMCs from our patient and healthy volunteers were incubated with LPS (1  $\mu$ g/mL) (Sigma-Aldrich) at a concentration of  $1 \times 10^6$  cells/mL at 37°C for 24 h. The concentration of TNF $\alpha$  in supernatant was measured using human BD OptEIA enzyme-linked immunosorbent assay kits (Becton-Dickinson, USA).

### Mutation Analysis and Reversion Analysis

Genomic DNA from our patient and his mother was extracted from PBMCs, stimulated T cells, and stimulated monocytes using Puregene DNA purification kit (Gentra/Qiagen, USA); total RNA was extracted using TRIzol, according to the manufacturer's instructions (Invitrogen, USA). Complementary DNA (cDNA) was synthesized from total RNA with TaKaRa RNA PCR<sup>TM</sup> Kit (AMV) (Takara, Japan). Polymerase chain reaction (PCR) of genomic DNA and cDNA was performed using TaKaRa LA Taq (TaKaRa) with primers to amplify between exon 2 and exon 4 in the *IKBKG* gene. PCR primers were as follows: c1F, 5'-GCGCTCCTGAGACCCTCCAG-3'; c2R, 5'-GAGGAGAAGGAGTTCCTCAT-3'; G3F, 5'-CCCAGCTCCCCTCCACTGTC-3'; G4R, 5'-AACCCCTGGAAGGGTCTCCGGAG-3'. Genomic DNA was denatured at 94°C for 3 min, followed by 35 cycles of denaturation at 94°C for 30 s, annealing at 64°C for 30 s, and elongation at 68°C for 2 min 30 s, and a final extension for 7 min at 72°C using G3F and G4R primers. cDNA was denatured at 94°C for 1 min, followed by 35 cycles of denaturation at 94°C for 30 s, annealing and elongation at 68°C for 1 min, and a final extension for 5 min at 68°C using c1F and c2R primers. After gel electrophoresis and visualization, targeted bands were extracted and sequenced using ABI Big-Dye Terminator (Applied Biosystems, USA).

To analyze the reversion of mutation, we used our X-EDA-ID patient's PBMCs and stimulated cells. Mononuclear cells sorted with FACSVANTAGE (Becton-Dickinson) were used only at analysis after 12 months of infliximab treatment. PCR products were subcloned using a TOPO

TA cloning kit (Invitrogen) and sequenced as described above.

#### Reporter Assay for Detecting a Mutant NEMO Function: NEMO-NF- $\kappa$ B Luciferase Reporter Assay

NEMO cDNAs from a healthy volunteer and our patient were subcloned into the p3xFLAG-CMV14 vector (Sigma), respectively. NEMO null rat fibroblast cells (kindly provided by Dr. S. Yamaoka) were plated at a density of  $3 \times 10^4$  cells/well in a 24-well culture dish and were transfected with 200 ng of plasmid, containing 40 ng of NF- $\kappa$ B reporter plasmid (pNF- $\kappa$ B-Luc; BD Biosciences Clontech, USA), 2 ng of a *NEMO* mutant expression construct, 148 ng internal control for normalization of transfection efficiency (pRL-TK; Toyo Ink, Japan), and the corresponding mock vector, using the FuGENE<sup>®</sup> HD Transfection Reagent (TOYO-B-Net, Japan) according to the manufacturer's protocol. At 12 h after transfection, the cells were stimulated with 15 ng/mL LPS for 4 h and the NF- $\kappa$ B activity was measured using the PicaGene<sup>®</sup> Dual SeaPansy assay kit (TOYO-B-NET) according to the manufacturer's protocol. Experiments were performed in triplicate and firefly luciferase activity was normalized to Renilla luciferase activity.

#### V $\beta$ and V $\alpha$ Analysis of T Cells

T cell receptor (TCR)  $\beta$  and  $\alpha$  chain variable region (V $\beta$  and V $\alpha$ ) repertoires were analyzed by a reverse transcription polymerase chain reaction (RT-PCR) method as described [16]. Briefly, each V $\beta$  fragment (from V $\beta$ 1 to V $\beta$ 20) or V $\alpha$  fragment (from V $\alpha$ 1 to V $\alpha$ 18, V $\alpha$ 21, and V $\alpha$ 24) was prepared from a series of HBVT/HBVP or HAVT/HAVP plasmids originating from thymus or peripheral T cells [17] and was dotted on filters. PCR products obtained from the patient by RT-PCR were labeled by  $\alpha$ -<sup>32</sup>P-dCTP and hybridized to the filters. Using densitometry, a semiquantitative assessment of V gene usage was made from the amounts of hybridized products.

#### Flow Cytometry

Peripheral blood samples were analyzed by three-color flow cytometry. Cells were stained with monoclonal antibodies to the following cell surface markers: CD3, CD4, CD8, CD19 (Becton-Dickinson), and CD14 (eBioscience, USA). Flow cytometry analysis of intracellular NEMO protein was performed as described previously [18]. Flow cytometric data from the stained cells were collected by FACScalibur and analyzed with CellQuest software (Becton-Dickinson).

#### Intracellular Cytokine Staining

Whole blood samples from our X-EDA-ID patient and healthy donors were stimulated with 1- $\mu$ g/mL ionomycin (Sigma-Aldrich) and 25-ng/mL phorbol 12-myristate 13-acetate (PMA) (Sigma-Aldrich) in the presence of 10- $\mu$ g/mL brefeldin A (Sigma-Aldrich) for 4 h. Cultured cells were stained with monoclonal antibodies against CD4 and CD8 for 30 min at room temperature. Stained cells were fixed and permeabilized with BD Lysing solution (Becton-Dickinson) and incubated with anti-TNF $\alpha$  monoclonal antibody or IgG1 isotypic control (Becton-Dickinson). Cells were analyzed by flow cytometry as described above. Analysis of intracellular TNF $\alpha$  in CD14+ cells was performed after stimulation with LPS (1  $\mu$ g/mL) at 37°C for 4 h.

#### Endoscopy and Immunohistochemical Staining

Endoscopy was performed with the consent of legal guardians. Colon biopsies were obtained at regions of visual abnormalities. Formalin-fixed paraffin-embedded tissues blocks were cut into 2- $\mu$ m sections and stained with hematoxylin and eosin. Subsequently, immunohistochemical analysis using the following primary antibodies with optimized experimental protocols was performed: CD3 $\epsilon$  (DAKO, Denmark, rabbit, polyclonal, diluted 1:100, incubated for 24 h at 4°C after microwave heat-induced antigen retrieval for 40 min in pH 6.0 citrate buffer), CD79a (DAKO, mouse, monoclonal, 1:100, microwave for 40 min, pH 6.0), CD68 (DAKO, mouse, monoclonal, 1:50, proteinase K (DAKO) for 10 min at room temperature), CD4 (Novocastra, USA, 1:100, microwave for 40 min, pH 9.0 (NICHIREI BIOSCIENCES, Japan)), CD8 (DAKO, mouse, monoclonal, 1:100, microwave for 40 min, pH 9.0), and TNF $\alpha$  (Santa Cruz Biotechnology, USA, goat, polyclonal, 1:200, microwave for 40 min, pH 6.0). An Envision-HRP Detection kit (DAKO) was used for visualization, except for anti-TNF $\alpha$ , which was visualized using donkey biotin conjugated anti-goat secondary antibody (Jackson ImmunoResearch Laboratories, USA) and LASB2-System/HRP kit (DAKO).

#### Infliximab Treatment

Infliximab treatment for our X-EDA-ID patient was approved by the medical ethics committee of the University of Miyazaki. We obtained written consent concerning treatment from both the patient and his guardian. Before initiating infliximab, we confirmed that he had no severe infection including tuberculosis according to laboratory data, mycobacterium culture test, skin tuberculin test, and chest computed tomography. Cardiac dysfunction was excluded by echocardiography and electrocardiogram.